Journal of Structural Geology, Vol. 11, No. 1/2, pp. 211 to 230, 1989
Printed in Great Britain

0191-8141/89 $03.00 + 0.00

Anatomy of mushroom-shaped diapirs

M. P. A. JACKSON

Applied Geodynamics Laboratory, Bureau of Economic Geology, The University of Texas at Austin, Austin, TX 78713, U.S.A.

and

C. J. TALBOT

Hans Ramberg Tectonic Laboratory, Institute of Geology, University of Uppsala, Box 555, S-751 22, Uppsala, Sweden

(*Received* 10 *May* 1988; *accepted* 12 *August* 1988)

Abstract—We produced more than 100 mushroom-shaped diapirs in eight centrifuged models under acceleration of 1200 *g*. The modelling results allow natural examples to be recognized. Mushroom diapirs have an overhanging bulb fringed by one or more skirts, which can curl inward to form vortices capable of entraining cover material to various degrees. Most of the internal folds are downward-facing. The oldest buoyant unit occurs in the skirt and in the diapiric core; younger buoyant units or their immediate cover are infolded in crescentic patterns. External mushroom diapirs have skirts that infold cover material. With greater maturity the skirts can curl inward to form an external vortex entraining cover. In contrast, internal mushroom diapirs have skirts confined entirely within the intrusion. Again, with greater maturity these confined skirts may curl inward, but they entrain only diapiric material. Internal mushroom structure results from toroidal circulation confined within the diapir, where isoviscosity prevails. External mushroom structure results where source and entrained cover have similar effective viscosities. Entrained inclusions of more-permeable country rock threaten the integrity of a mined cavern by creating a plumbing system.

INTRODUCTION

THE term 'mushroom-shaped' has previously been loosely applied to any model or natural diapir shaped like a light bulb, despite the fact that actual mushrooms are not shaped like this. Mushroom-shaped diapirs (hereafter called 'mushroom diapirs') have a broad bulb (overhanging swollen crest) fringed by one or more laterally flattened *skirts* which envelop the lower part of the bulb. We restrict the term 'mushroom diapir' to those with skirts, regardless of the size, shape or number of these pendant lobes.

Mushroom diapirs were produced in numerical models by Daly (1967), Berner *et al.* (1972), Woidt (1978, 1980) and Schmeling (1987). Mushroom diapirs have also been physically modelled (Talbot 1974, 1977, Dixon 1975, Whitehead & Luther 1975, Ramberg 1981). Ramberg (1981, pp. 309–314) modelled the internal structures of diapirs, and although these did not include mushroom shapes, his study inspired us to explore the topic. The anatomy of mushroom diapirs has never been studied in detail, nor, with rare exceptions, has their existence even been established in nature.

Several reviews have addressed internal structure of salt diapirs at mesoscopic and microscopic scales on the basis of detailed study of small parts of mined salt stocks (for example, Kupfer 1968, Richter-Bernburg 1980, Jackson 1985, Talbot & Jackson 1987a). In contrast we document the occurrence and macroscopic geometry of entire mushroom diapirs in centrifuge experiments, illustrate natural examples and discuss controls on their formation in experiment and nature. Here we explore a field of structural geology that, as far as we are aware, has never been previously studied: interference structures in axisymmetric (rather than cylindrical) fold systems.

An understanding of mushroom structure has significant practical benefits with respect to the exploitation of evaporite ores, to the storage of hazardous or useful materials in diapirs and in exploration for oil and gas around the flanks of diapirs. This paper emphasizes salt diapirs, but the results are also potentially applicable to diapirs of shale, peat, granite, gneiss and serpentinite. The natural examples of mushroom diapirs described here are all evaporitic. We are preparing a companion paper dealing with mushroom diapirs in igneous and gneissic terrains.

This research was part of a larger program of centrifuge experiments conducted by the authors at the Hans Ramberg Tectonic Laboratory at the University of Uppsala, Sweden. Procedures for designing, constructing and centrifuging these models are documented in Jackson & Cornelius (1987) and Jackson *et al.* (1988).

FACTORS CONTROLLING THE SHAPE OF MUSHROOM DIAPIRS

During diapiric upwelling, downward drag by the surrounding cover and upward drag by the core of the

rising diapir mean that buoyant material near the periphery of the diapir rises more slowly than the core. This sets up viscous toroidal circulation, whose stream surfaces are centered on the core of the bulb and are concentric about a horizontal, circular axis. In response to this isothermal circulation, the crest of the diapir widens to form a bulb. With sufficient maturity this flow is recorded by internal folds within the bulb.

Theoretical and experimental studies show that the shape of the diapir bulb depends largely on the parameter m: the ratio of the viscosity of the overburden divided by the viscosity of the source layer (Berner *et al.* 1972, Whitehead & Luther 1975, Heye 1978, 1979, Woidt 1978, 1980). Effective viscosity, which is the dynamic shear viscosity applicable in a particular situation, refers here to the strain rate of a rock under particular conditions or at a particular stage of development. The diapir shape and the relative involvement of the diapiric material and its cover relate to m, how far the diapir has risen and to the proximity of neighboring diapirs (Schmeling *et al.* 1988).

Figure 1 illustrates the tendency of toroidal circulation to shift progressively inward as m increases. Three morphological types of bulbs have been differentiated as types A, B and C (Jackson & Talbot 1986, Talbot & Jackson 1987a, b). Where $m \ll 1$, relatively widely spaced type A diapirs swell to thumblike shapes (Fig. 1), and toroidal circulation occurs mainly in the cover because it is softer than the source layer.

In contrast where $m \gg 1$, closely spaced type C spherical blobs are generated because the circulation occurs mainly within the softer diapir (Fig. 1). Balloon-like blobs rise faster than the stems, which thin to tenuous threads and rise from pronounced withdrawal basins in the source layer. Toroidal circulation can lead to more than one overturn of the diapiric sequence in bulbs that rise significant distances, forming a vortex at the highly mature stage. Whether the bulb detaches in evaporite diapirs (as in magmatic plutons) is uncertain, but the detached bulb in models is spherical if the surrounding fluid exhibits Newtonian flow behavior. Conversely, the base of the bulb elongates like an inverted teardrop if the surrounding fluid exhibits power-law behavior (van Dyke 1982, figs. 182 and 183).

Where m is within an order of magnitude of 1, both cover and source circulate toroidally, forming a type B mushroom-shaped bulb trailing a skirt (Fig. 1). The cover is infolded from below. The skirt does not sink relative to the source layer; it merely rises more slowly than the core of the diapir. Numerical and physical modelling indicates that type B mushroom bulbs are most likely to form in crowded diapirs that incorporate closely spaced initial irregularities and that rise through thick aggrading cover (Schmeling 1987).

Where the cover is as thick as or thinner than the source layer, diapirs cannot rise sufficiently for these differences to become obvious, and all types of bulbs tend toward a squat, broad balloon shape (Woidt 1978, 1980).

Figure 2 shows the two classes of mushroom diapir.

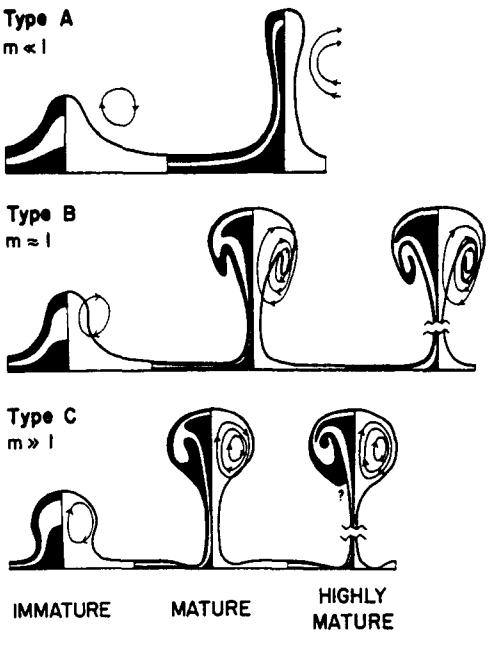

Fig. 1. Schematic effects of viscosity contrast on shapes of diapirs based on physical and numerical modelling by Berner *et al.* (1972), Whitehead & Luther (1975), Heye (1978, 1979) and Woidt (1978, 1980) and on unpublished experiments at the University of Uppsala. Stripes in the left-hand side of each upwelling depict a three-layer stratigraphy. Loops on the right-hand side of each upwelling represent toroidal streamlines viewed in a reference frame centered on the rising bulb. The variable, m, is the effective viscosity ratio between cover and source layer. Immature domes show subtle but recognizable differences that increase with maturity. At maturity, type B and C bulbs have simple mushroom structure; by the highly mature stage, these can evolve into vortex mushroom structure. The highly mature stage of type A bulbs is similar to that shown for the mature stage.

Diapirs with infolded cover have *external mushroom structure:* here $m \sim 1$, the bulb is type B, toroidal circulation entrains cover as well as diapiric material and the diapir's contact becomes invaginated into the base of the bulb. In contrast, mushroom diapirs in which only the diapiric sequence is infolded or coiled have *internal mushroom structure* (Fig. 2): here $m > 10$, the bulb is type C, toroidal circulation is entirely internal, and the contact is not invaginated.

GENERAL ANATOMY OF CENTRIFUGED MUSHROOM DIAPIRS

Figure 3 shows the original configuration and material properties of eight models before acceleration in a centrifuge. The models were constructed from silicone putty and modelling clay mixtures. Multilayers of contrasting color simulated bedding and revealed the internal deformation of the diapirs. These strain markers were mechanically inactive. Between 10 and 20 domes were typically produced in each model (Fig. 4). In Figs. 5–14 actual sections through models are identified by a six-digit model number: graphically constructed sections are indicated by the absence of a model number. Edge effects at their boundaries control the shape of centrifuged diapirs. The origin of these edge effects has been discussed previously (Jackson & Cornelius 1987,

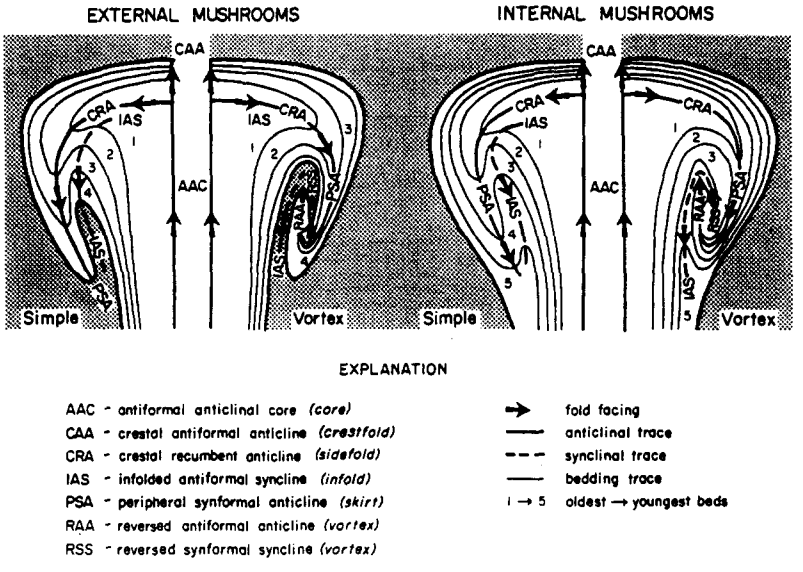

Fig. 2. Two classes and four types of mushroom diapirs shown schematically in vertical half-section together with the terminology and acronyms of second-order folds; the informal terms in italics are generally used in the text. The sedimentary cover is stippled. External mushroom diapirs have a type B bulb. Internal mushroom diapirs have a type C bulb. For both types of bulbs, the simple mushroom structure can evolve to a vortex mushroom structure if the skirt curls inward and upward to an upward-facing orientation (cf. Fig. 1).

Jackson *et al.* 1988). Asymmetry in salt diapirs results from several causes, such as edge effects, diapiric rise from a tilted source layer, mutual interference between growing diapirs, gravity spreading of cover, tangential stress and uneven sedimentary loading (Talbot 1977, Jackson & Cornelius 1987).

Decorating the first-order structural dome of a mushroom diapir are the second-order major folds investigated here. These folds are defined by initially horizontal multilayers. Even in the simplest centrifuged dome, the second-order fold system is complex (Fig. 5). Because of this complexity, we did not attempt to superimpose additional complications also present in nature, such as dissolution or faulting. The crests and shoulders of salt diapirs are typically truncated by erosion or subsurface solution, leaving a carapace of cap rock as the insoluble residue.

Flow within the mushroom diapirs in Figs. 2 and 5 can be traced by the orientation of the second-order folds. Buoyant material rises up the stem and through the *core* of the bulb, spreads laterally at its crest, then flows downward (relative to the core) at the margins, forming a skirt. Between the skirt and the core is an *infold* of cover.

Figure 2 shows the formal terminology and the three-letter acronyms referring to these folds. We use this formal terminology in the diagrams to correlate folds in different diapirs but in the text only where necessary for precision. Except for the synclinal infold, these second-order folds are anticlinal. Both the infold and the skirt are downward-facing folds. The skirt is a synformal anticline, and the infold is an antiformal syncline. The axial trace of the PSA skirt passes upward and inward via the CRA into the axial trace of the AAC. Their axial traces are concentric in plan view, so the PSA and IAS can each appear twice in vertical section (Fig. 2) because they are single structures linked horizontally.

The immature development of most of these major folds was simulated by Dixon's (1975) centrifuged models, which contained passive marker layers similar to our own. Although the folds were not specifically labelled as such, the AAC core and the CAA and CRA folds are present in all his models. In addition, his gneiss-dome model, WD-3, also contains an embryonic downward-facing IAS infold and PSA skirt defined by bedding parallel layering; $m = 0.23$ in this model, indicating that a mushroom diapir can form where the viscosity contrast is not precisely unity, but that its mushroom character is subtle even though the diapir as a whole has an extremely broad bulb.

The number of second-order folds intersected across the diameter of the mushroom diapir can be used to classify members of this family. Figure 6 shows a non-inclusive variety of mushroom structures to illustrate this n-fold classification. To distinguish them from the more complex vortex diapirs, the non-vortex mushroom diapirs are termed *simple*. Symmetric diapirs have the same number and type of major folds on each side of the diapiric core. We use the term 'symmetric' loosely and ignore the size and shape of the major folds. These are invariably different on each side of a centrifuged diapir or natural diapir although they can be identical in mathematical models.

The three-dimensional structure of mushroom diapirs is considerably more complex than their appearance in vertical section. Both external fivefold mushroom diapirs in Fig. 7 yield vertical sections like the leftmost part of Fig. 2, but their horizontal sections are quite different. Figure 7(a) shows a horizontal section through an axially symmetric fivefold diapir. Figure 7(b) shows

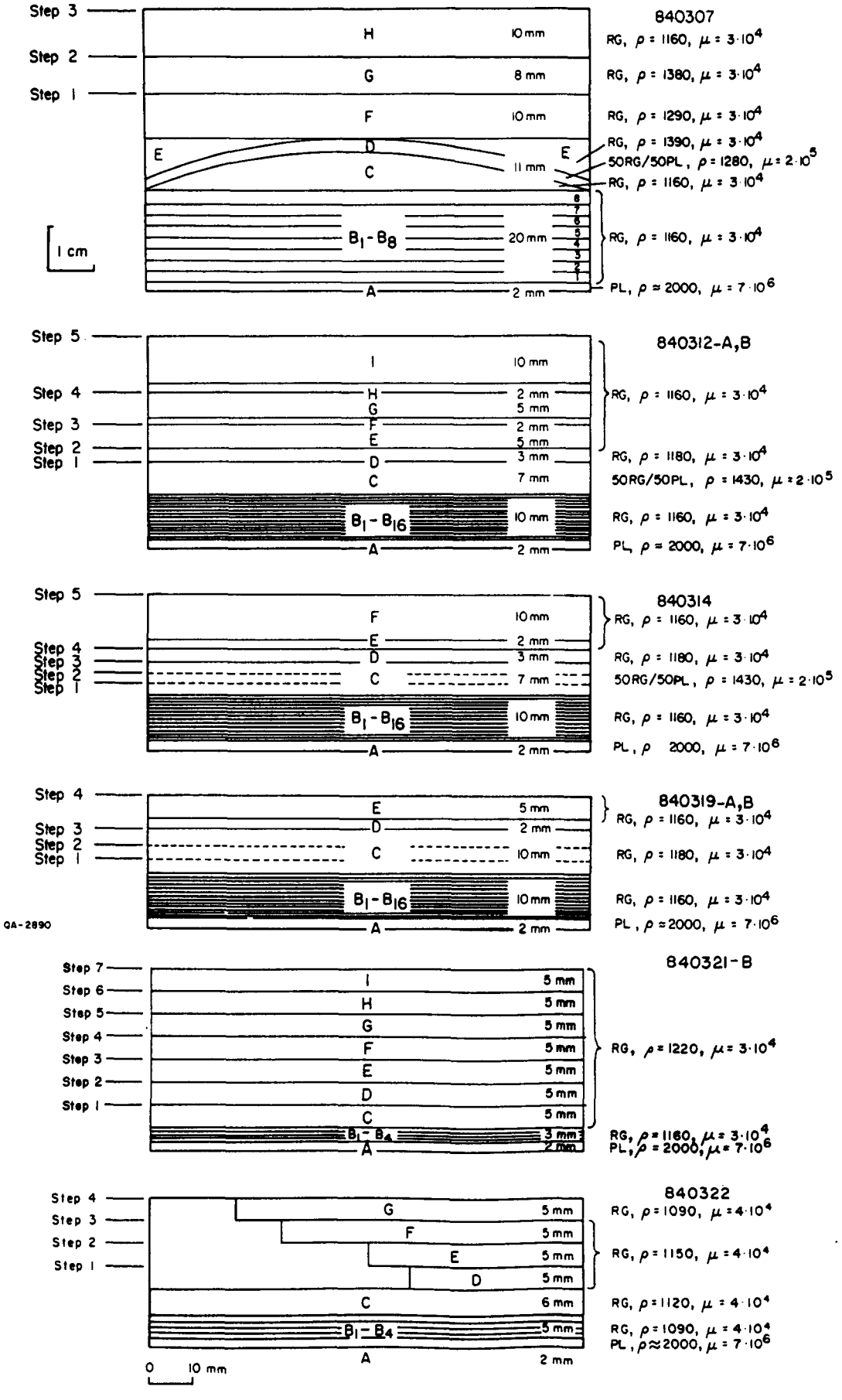

Fig. 3. Vertical sections showing the original configuration of eight models (including twins for 840312 and 840319) before acceleration in a centrifuge. Centrifuged diapirs 840307, 840312-A, 840314, 840319-A, 840321-B and 840322 grew during incremental addition of cover (downbuilding). Steps refer to levels at which new layers were incrementally added between centrifuge runs. Diapirs in 840312-B and 840319-B began growing after all the cover layers were in place (upbuilding). The source layer, B, is divided into four, eight or 16 multilayers as shown. ϱ is density (kg m^{-3}); μ is effective viscosity (Pa s); RG is Rhodorsil Gomme (silicone putty), PL is Plastilina (modelling clay), 50 RG/50 PL is a mixture of 50 weight per cent RG and 50 weight per cent PL; densities were increased by adding $BaSO_4$ powder. (From Jackson *et al.* 1988, except for 840322.)

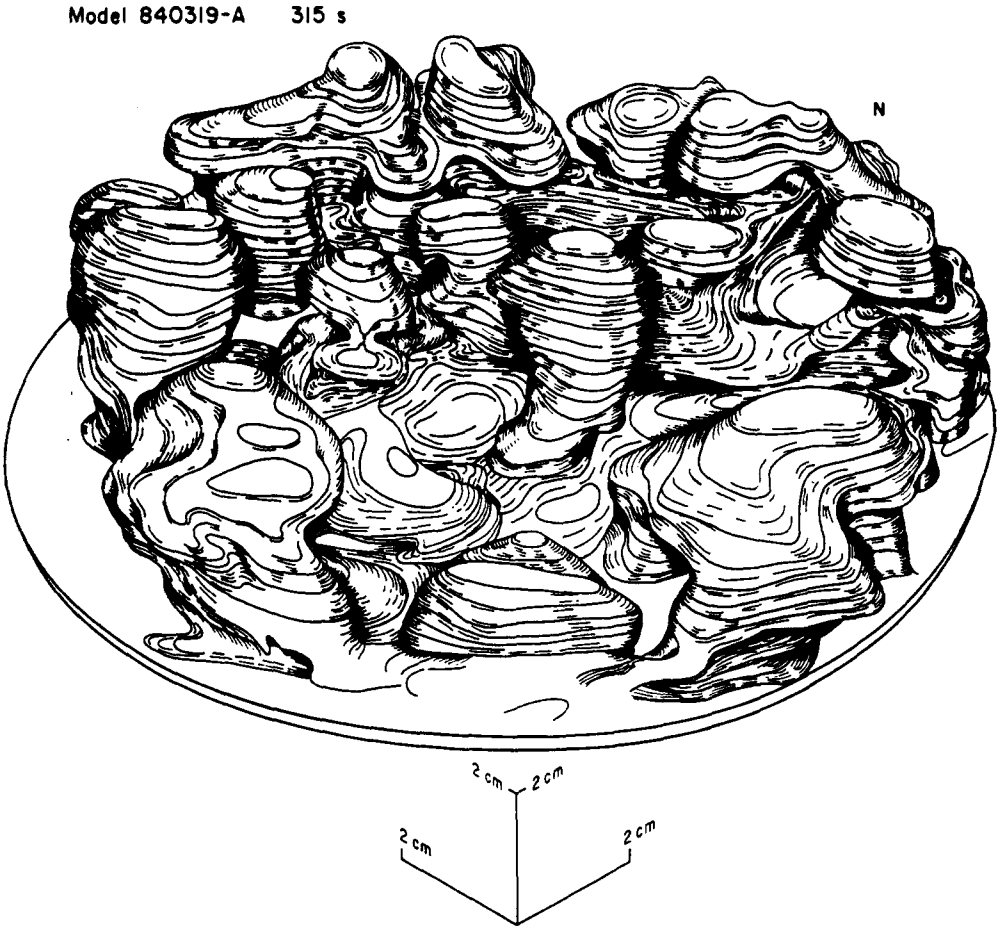

Fig. 4. Isometric diagram of the upper surface of the source layer in model 840319-A. All the diapirs contain at least one skirt, and some have two, although the narrow lower skirt is not readily apparent without sectioning. The diagram was constructed from data obtained from vertical and horizontal slices through the model; the cover is not shown for clarity. Contour interval is 1.25 mm. N is an arbitrary reference direction.

an orthorhombic diapir. Arbitrarily designating north toward the top of the figure, its skirt is lowest in the northeast and southwest, whereas the infold is highest in the northwest and southeast. The resulting crescentic closed fold patterns in Fig. 7(b) characterize horizontal sections through tilted or irregular diapirs. A concise alternative term for the second-order folds in mushroom diapirs is thus 'crescentic'.

Of course, fold patterns in horizontal section depend on the structural level within the diapir, and not all horizontal sections contain crescentic fold patterns. A horizontal section through the crestfold or stalk (Fig. 2) shows only a simple dome, represented by a bull's eye pattern.

These crescentic folds are not to be confused with the curtain folds (*Kulissenfaltern*) described in German and U.S. salt domes (e.g. Stier 1915, Escher & Kuenen 1929, Balk 1949, Ahlborn & Richter-Bernberg 1953, Kupfer 1968). They differ in origin, geometry and size. Crescentic folds originate within the bulb of a diapir, whereas curtain folds form primarily by constriction of the underlying stem by amplification and rotation of deep polygonal ridges connecting the bases of diapirs. The crescentic fold hinges are generally shallow plunging, and their axial traces are concentric. In contrast curtain folds are generally steeply plunging with radial axial traces. Crescentic folds can be subtle and difficult to recognize in horizontal section but comparatively obvious in vertical section. The opposite is true for curtain folds.

ANATOMIES OF SPECIFIC CENTRIFUGED MUSHROOM DIAPIRS

All threefold diapirs are asymmetric (Figs. 6 and 8). The core is near the side of the diapir, the skirt (which only partly envelops the core) is near the opposite side, and the infold tends to be centered.

The ideal shapes of fivefold diapirs illustrated in Figs. 6 and 7 were not produced in our models, but the fivefold centrifuged diapirs are nevertheless symmetric in the broad sense we have defined.

Figure 9 shows a fivefold diapir in vertical section and in three horizontal sections at different levels. The central horizontal section shows a complex fivefold structure. Two crescents arranged back-to-back in horizontal section represent the core. The arms of the crescents merge into a skirt, which encircles two infolds. The sections above and below show threefold structure. The core switches position between the levels of the two

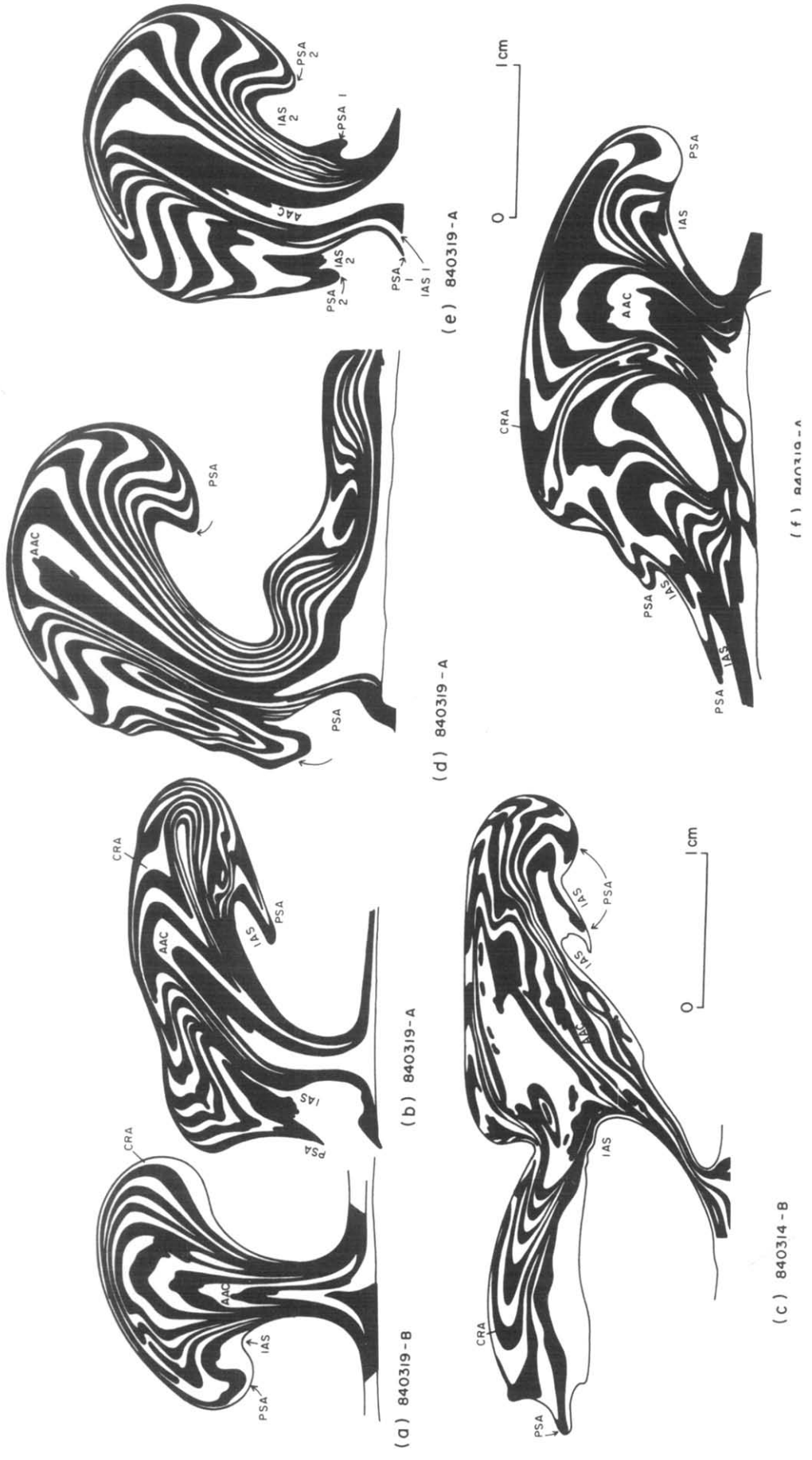

Fig. 5. Actual vertical sections through a variety of centrifuged diapirs. Alternating black and white multilayers are passive markers. AAC, antiformal anticlinal core; CRA, crestal recumbent anticline; PSA, peripheral synformal anticline (skirt); IAS, infolded antiformal syncline (infold). (a) Asymmetric diapir with skirt and infold on the left-hand side and simple overhang on the right-hand side. (b) Symmetric tilted diapir with highly mature bulb. (c) Complex diapir whose bulb appears to be unusually broad because the slice includes a peripheral diapir wall on the left, which is an edge effect; the bulb overhang is actually greater on the right-hand side. (d) Symmetric tilted diapir with peripheral lobe at different levels on each side; drag by the model wall to the left retarded the rise of the diapir bulb, causing a lower skirt on the left. (e) Double skirts on each side of a symmetric diapir; the left side of the lower spurlike skirt (PSA 1) was greatly flattened by flow of cover toward the diapir stem. (f) Two diapirs fused to form a composite bulb over a double stalk; the right diapir bulb extends over the left diapir bulb.

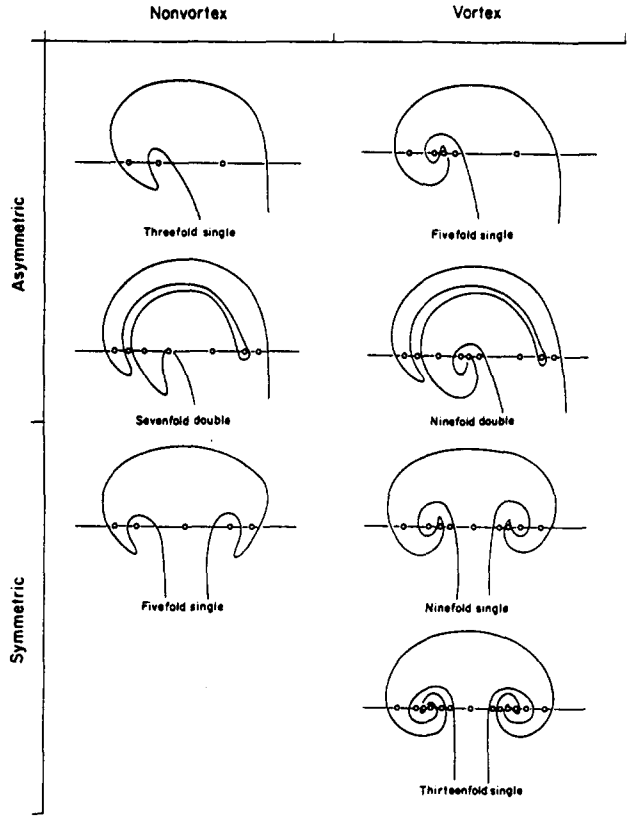

Fig. 6. Nomenclature of schematic mushroom diapirs in vertical section. Circles mark the intersection of second-order axial traces (not shown) with a horizontal plane (thin, straight line). The number of intersections across the complete dome diameter determines the *n*-fold diapir classification.

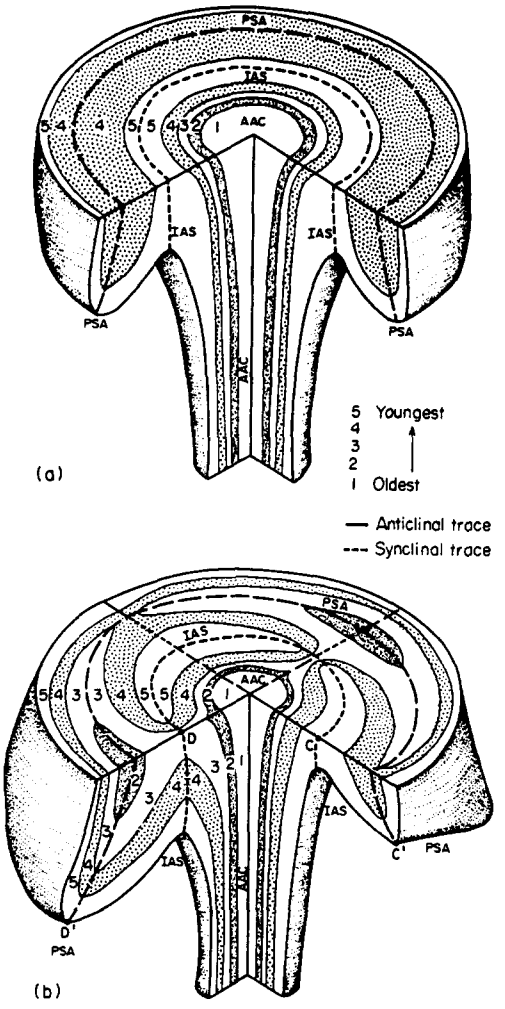

Fig. 7. Isometric diagrams of hypothetical fivefold diapirs showing the relation between two vertical sections and a horizontal section above. (a) Axially symmetric diapir. (b) Orthorhombic symmetric diapir cut along the two planes of symmetry. Points D and D′ mark the depression points of the infold and skirt, whereas C and C′ mark the culmination points of these folds, respectively. AAC, antiformal anticlinal core; PSA, peripheral synformal anticline (skirt); IAS, infolded antiformal syncline (infold).

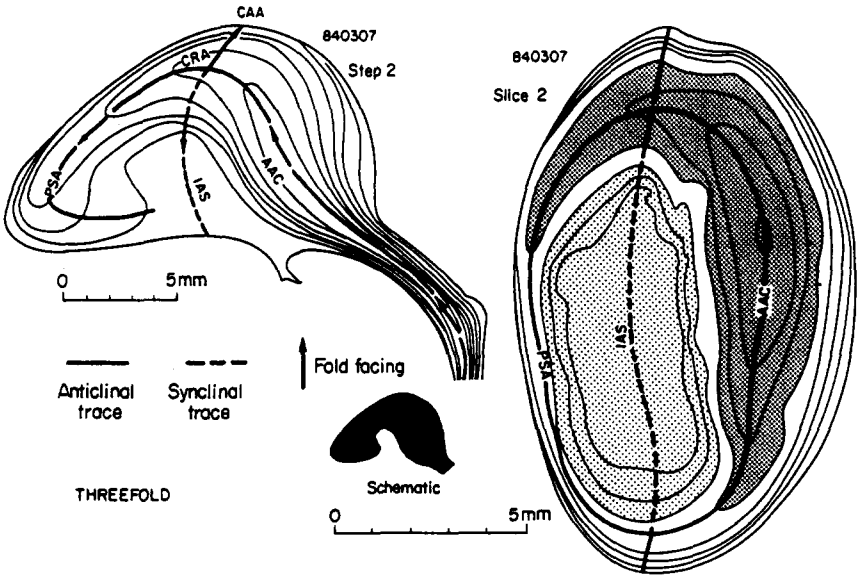

Fig. 8. Actual vertical (left) and horizontal (right) sections through two centrifuged threefold asymmetric diapirs. Arbitrary multilayers are stippled to emphasize the closed fold patterns in horizontal section. ACC, antiformal anticlinal core; CAA, crestal antiformal anticline; CRA, crestal recumbent anticline; PSA, peripheral synformal anticline (skirt); IAS, infolded antiformal syncline.

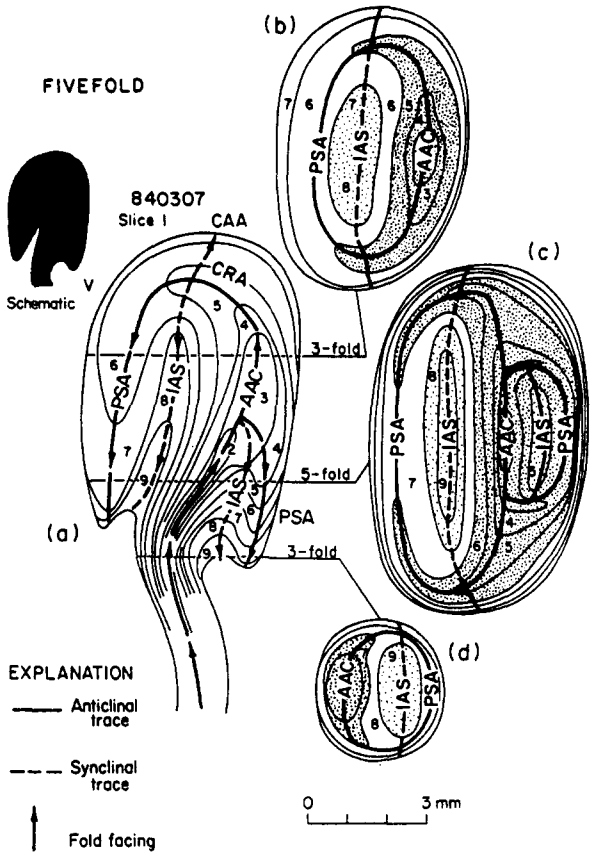

Fig. 9. Sections through a centrifuged fivefold symmetric diapir. (a) Actual vertical section. (b)–(d) Constructed horizontal sections drawn for three different structural levels that are labelled to the right of (a). Multilayer 2 is the oldest and 9 is the youngest. Arbitrary multilayers are stippled to emphasize the closed fold patterns in horizontal sections. AAC, antiformal anticlinal core; CAA, crestal antiformal anticline; CRA, crestal recumbent anticline; PSA, peripheral synformal anticline (skirt); IAS, infolded antiformal syncline.

threefold structures. Even higher or lower sections (not illustrated) have onefold structure—a simple bull's eye.

Sevenfold double diapirs can be produced in two ways:

(1) by lateral fusion of the bulbs of two similar diapirs. Fusion is more likely where diapirs grow syndepositionally (known as downbuilding) because the characteristic wavelength of diapirism lengthens in response to the thickening cover (Jackson *et al.* 1988). The result is two discrete diapir stalks and a single bulb having sevenfold internal structure overall (Fig. 5f). Each stalk is separated by cover that defines an antiformal synclinal core (ASC) and a synformal synclinal core (SSC) (Fig. 10). The ASC of cover projects deep into the diapir bulb;

(2) by non-coeval growth of dissimilar asymmetric diapirs. This results in a structure that resembles in vertical section a human arm draped across a head (Fig. 11). The bulb of an older asymmetric diapir spreads laterally like a recumbent fold above a younger or slower diapir. The younger bulb rises into the recumbent older bulb, arching and stretching the older bulb (the draped arm) over the crest of the younger diapir (the head). A partition of infolded cover extends into the center of the composite diapir, dividing it into its component diapirs, and hence is known as a dividing syncline (DS). This is a downward-facing antiform (the dividing antiformal syncline, or DAS) near the periphery of the double diapir but is an upward-facing synform (the dividing synformal syncline, or DSS) at the base of the draped arm.

The elevenfold double diapir illustrated in Fig. 12 is one of the most complex structures we modelled. The two diapirs are separated by the dividing syncline (dashed line) in the three horizontal slices (Fig. 12, left column). The inner diapir is a sevenfold mushroom diapir. Its skirt, outlined by multilayer 3 (black in Fig. 12) is extremely attenuated because of an unusually thick cover: the cover-to-source thickness ratio is 12. The cover is about four times as thick as the deep bulbs are wide, thus allowing space for the bulbs to rise and develop to an advanced stage of maturation with an attenuated skirt. The laterally flattened, wall-like stem of the diapir splits near its end into two protruding buttresses, prominent in horizontal slices 7 and 8 (Fig. 12, along line of section). Infolded sideways between these buttresses is cover layer C, which thus appears in

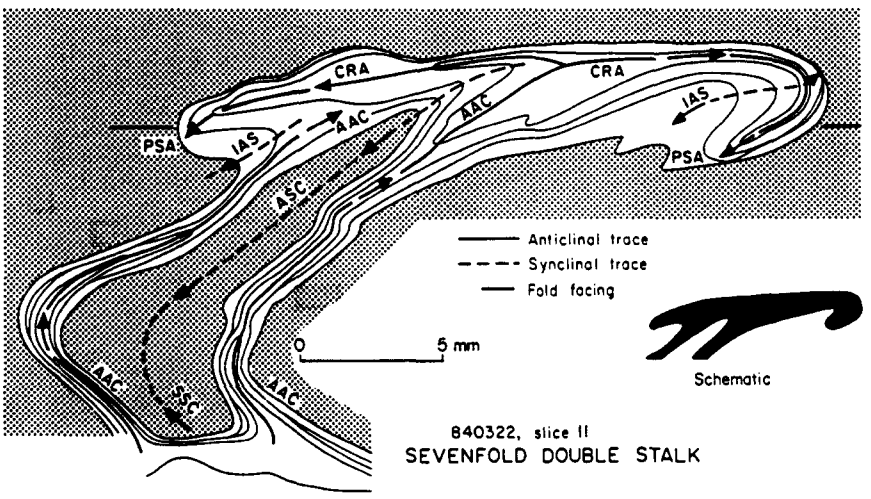

Fig. 10. Actual vertical slice of a centrifuged sevenfold symmetric double-stalk diapir formed by lateral fusion of the bulbs of two coeval diapirs. A core of cover (stippled) defines the antiformal synclinal core (ASC) and the synformal synclinal core (SSC). The ASC projects into the center of the bulb. AAC, antiformal anticlinal core; CRA, crestal recumbent anticline; IAS, infolded antiformal syncline; PSA, peripheral synformal anticline (skirt).

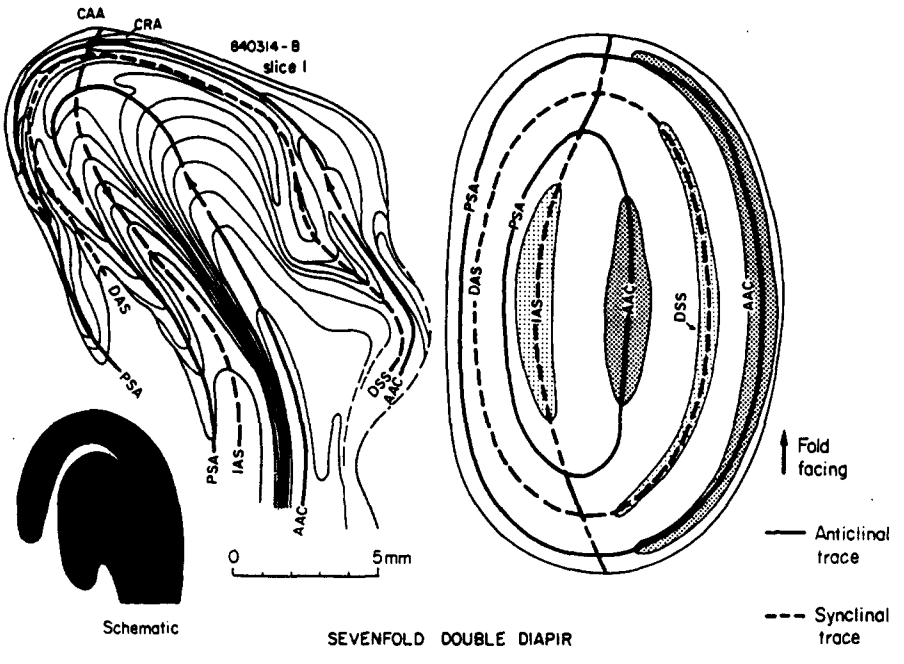

Fig. 11. Actual vertical (left) and constructed horizontal (right) sections through a centrifuged sevenfold asymmetric double diapir with a draped-arm structure shown schematically (lower left). Arbitrary multilayers are stippled to emphasize the closed fold patterns in horizontal section. AAC, antiformal anticlinal core; CAA, crestal antiformal anticline; CRA, crestal recumbent anticline; DSS, dividing synformal syncline; DAS, dividing antiformal syncline; IAS, infolded antiformal syncline; PSA, peripheral synformal anticline (skirt).

the core of the vertical section as an antiformal synclinal core (ASC).

The inner diapir is shrouded by the skirt of an older, higher, recumbent diapir. The vertical section in Fig. 12 (right column) intersects this shroud at right angles to its spreading direction, so that the older diapir skirt resembles not a draped arm (as in Fig. 11), but a rootless crescent (Fig. 12, schematic section).

Vortex structures flanking diapir cores are common in models of thermal convection (Rayleigh–Bénard instability) driven by a thermal gradient and in models of diapirism due to density inversion (Rayleigh–Taylor instability) where inertial forces are much greater than viscous forces (Daly 1967). However, neither of these conditions applies to our centrifuged diapirs, and vortex structures have not been previously reported in centrifuged models. However, vorticity was present in one of our models (described below), so we offer an explanation involving viscous behavior with negligible inertia.

Vortex structures form if there is more than one overturn of diapiric material and, possibly, of cover entrained in second-order folds. The first overturn produces downward-facing folds such as the skirt and infold. As the diapir bulb expands sideways, sinking cover moves inward beneath it, molding the bulb into a downward-pointing cone. Continued viscous shear by the cover curves the downward-facing skirt inward. The hem of the recumbent skirt then enters the drag zone of the rising core and is entrained into a second overturn. The recumbent skirt and overlying infold are curled upward and refolded into an upward-facing orientation once more. We call the resulting structures *reversed upward facing* to distinguish them from upward facing structures like the AAC core that have not been inverted.

A hypothetical example of the simplest type of vortex structure is shown in Fig. 13. The diapir is an internal fivefold vortex mushroom. If a fivefold structure became coiled by vorticity, a ninefold vortex structure could form (Fig. 6). Such a structure has not yet been recognized in the centrifuged diapirs, but has in nature (see the section on Central Iran). Figure 14 shows a centrifuged sevenfold vortex structure in which a threefold diapir developed a coiled skirt on one side only; the other side was retarded by edge effects.

EVAPORITIC MUSHROOM DIAPIRS

This section describes four basins where natural evaporite diapirs contain folds recognizable as mushroom structures. Each diapir has at least internal mushroom structure and, in some cases, external mushroom structure. Natural diapirs have a highly irregular internal structure. Even in models constructed from homogeneous layers, the resulting diapirs are not axisymmetric because growing diapirs interfere with their neighbors. The inhomogeneous lithology and irregular deposition of natural sediments degrade the symmetry even further. The difficulty in interpreting the convoluted anatomy of salt domes is compounded by partial dissolution. Many of the German diapirs exemplify the difficulty of classifying some natural diapirs according to the *n*-fold system. Higher-order crescentic folds decorate the major crescentic folds in a spectrum of different sizes. Deciding which folds are

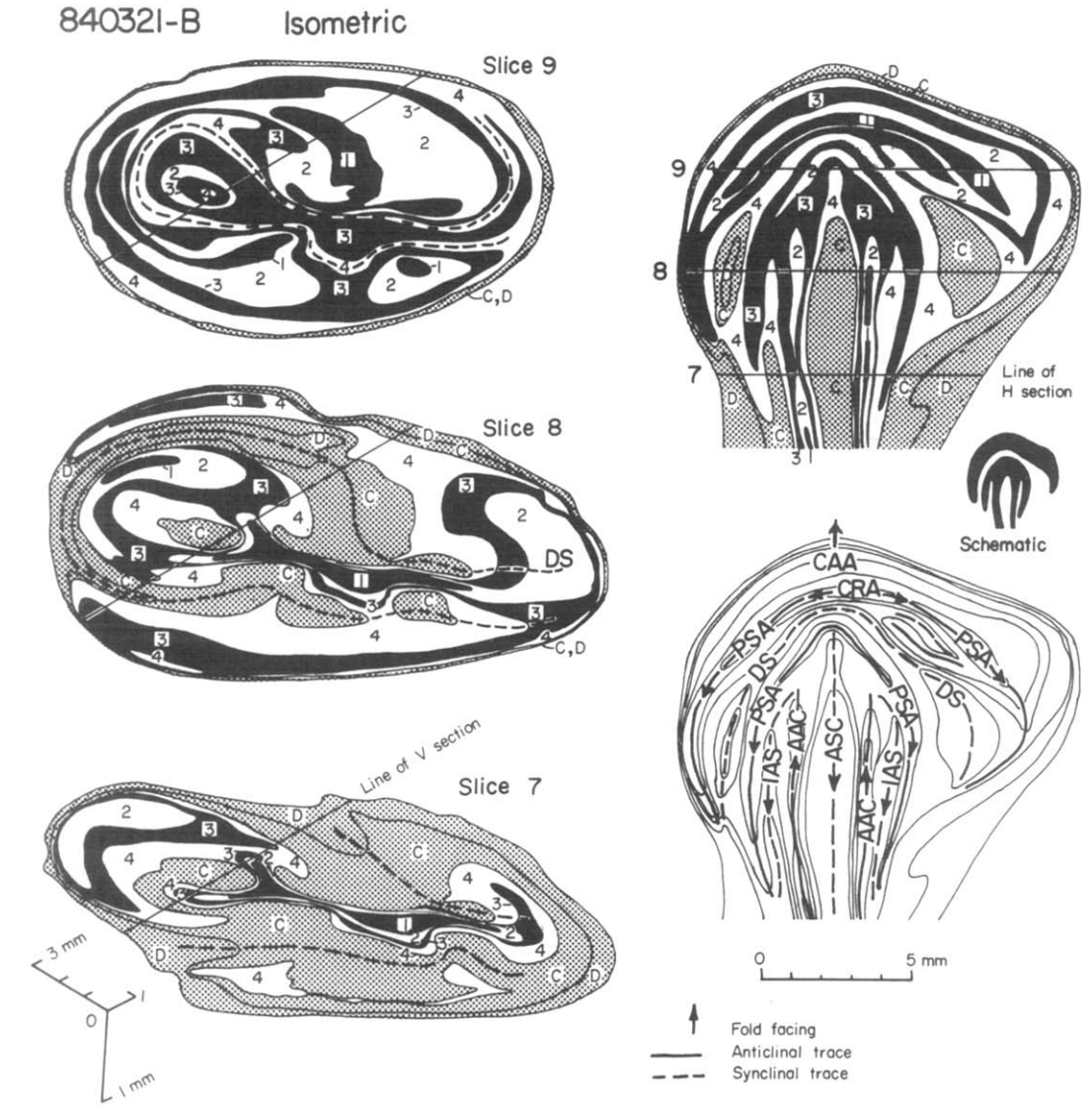

Fig. 12. A centrifuged elevenfold double diapir combining features of the diapirs in Figs. 10 and 11. Left column: isometric projections of actual horizontal slices in the same relative positions as in the unsliced model: the vertical spacing between the slices is exaggerated 3 times to prevent occlusion; identical line of section in each slice refers to the right column; dashed line is the trace of the dividing syncline (DS) separating an inner, younger, upright diapir from an outer, older, recumbent diapir. Right column: vertical section constructed without vertical exaggeration from five horizontal slices, three of which are numbered and refer to the left column; upper vertical section shows folded multilayers and layers, lower section shows fold interpretation. Black-and-white multilayers constitute the source layer B; they are numbered from 1, the oldest, to 4, the youngest. Cover layers C and D are stippled and younger cover layers are omitted for clarity. AAC, antiformal anticlinal core; ASC, antiformal synclinal core; CAA, crestal antiformal anticline; CRA, crestal recumbent anticline; IAS, infolded antiformal syncline; PSA, peripheral synformal anticline (skirt).

significant enough to affect the diapir's classification can be subjective. In assigning a diapir to a particular class, we counted the minimum number of crescentic folds required to define the structure.

Northwest German Plain

At least nine salt diapirs in Germany have internal mushroom structures, which were previously recognized in only two of them. The nine diapirs have plan shapes ranging from near-circular salt stocks to highly elongated salt walls. One of the salt walls is being used as a nuclear waste storage facility, and a second is being considered for such use, so an understanding of their internal structure is of more than academic interest. Eight of the diapirs have been mined (the effects of which have been omitted from our figures for clarity) for their potassium salts. Consequently their internal structure is defined by a consistent stratigraphy—generally comprising three of the seven cycles within the Permian Zechstein, abbreviated in order of decreasing age as *Z*2, *Z*3 and *Z*4.

Asse Dome (Fig. 15) has been mined for potash and salt since 1899. The abandoned Asse 2 mine stores low-level and intermediate-level nuclear wastes emplaced from 1967 to 1978 and is still used as an experimental facility for nuclear waste storage. Extensive mining on 20 levels has revealed the major folds in the crest of the diapir (Essaid & Klarr 1982). The folds

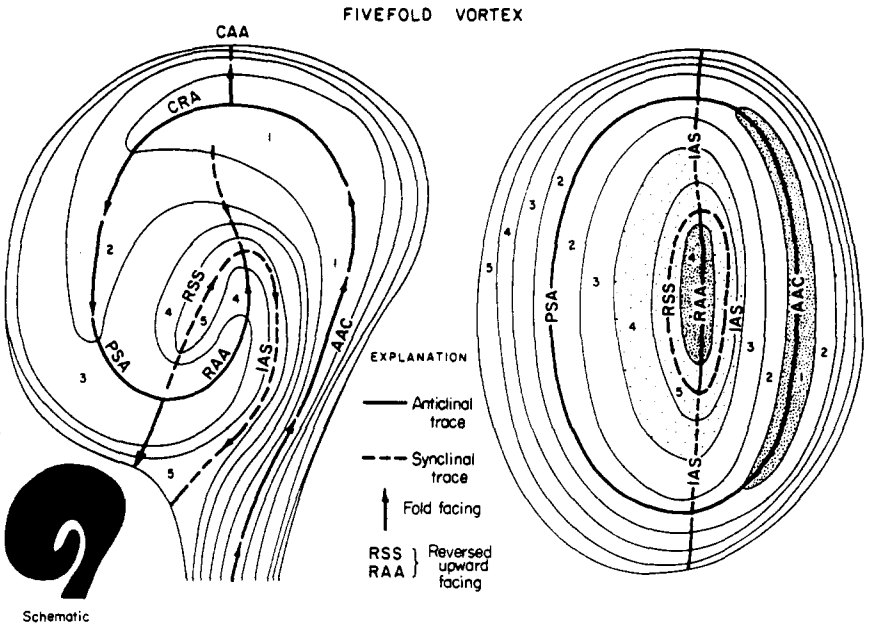

Fig. 13. Vertical (left) and horizontal (right) sections through a hypothetical fivefold asymmetric diapir with vortex structure. Numbers show stratigraphic sequence, with 1 being the oldest multilayer and 5 being the youngest. Arbitrary multilayers are stippled to emphasize the closed fold patterns in horizontal section. AAC, antiformal anticlinal core; CAA, crestal antiformal anticline; CRA, crestal recumbent anticline; IAS, infolded antiformal syncline; PSA, peripheral synformal anticline (skirt); RAA, reversed antiformal anticline; RSS, reversed synformal syncline.

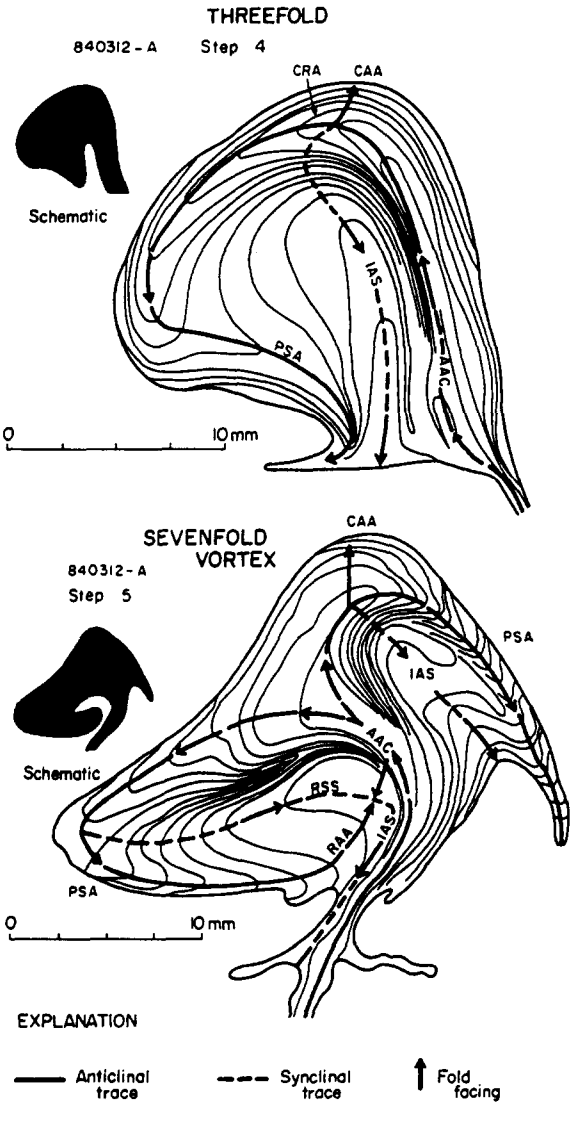

define a fivefold double diapir (two cores), the innermost of which has threefold asymmetry with a downward-facing infold and skirt. The dividing synformal syncline (DSS) comprises *Z*3 evaporites. The crestal antiformal anticline (CAA) of Asse Dome is a simple structure hiding the complexities below.

The well-explored elliptical Hänigsen Dome (Fig. 16) appears to have spread at the surface 80 Ma ago, before its crest was truncated by dissolution and erosion (Talbot & Jackson 1987a). The major fold hinges are subhorizontal in the upper part of the bulb and steepen downward into the stem (Richter-Bernburg 1980). Part of the complexity in Fig. 16 is due to steeply plunging curtain folds curving in and out of the plane of section through the stem. Because the core of the diapir stem is out of this plane of section, fold facing can be reliably inferred only in the bulb in the upper part of the diagram. As is typical of mushroom diapirs, most of the folds are downward facing (Fig. 16, axial traces). The upward-facing antiform cored by *Z*2, which was intersected by the Reidel shaft, is a significant exception. We suggest that the antiform is part of a very tight vortex structure, which has also entrained an isocline of *Z*4 (Fig. 16, stippled unit in main section). The inferred vortex is internal, so the effective viscosity of the country rock (Buntsandstein and Muschelkalk stratigraphic units) is probably significantly greater than that of the Zechstein salt (cf. Figs. 1 and 2).

Fig. 14. Actual vertical sections through two centrifuged diapirs at different stages of development. (Top) Mature threefold asymmetric diapir. (Bottom) Highly mature sevenfold asymmetric diapir with vortex in its left half resulting in upward-facing folds. AAC, antiformal anticlinal core; CAA, crestal antiformal anticline; CRA, crestal recumbent anticline; IAS, infolded antiformal syncline; PSA, peripheral synformal anticline (skirt); RAA, reversed antiformal anticline; RSS, reversed synformal syncline.

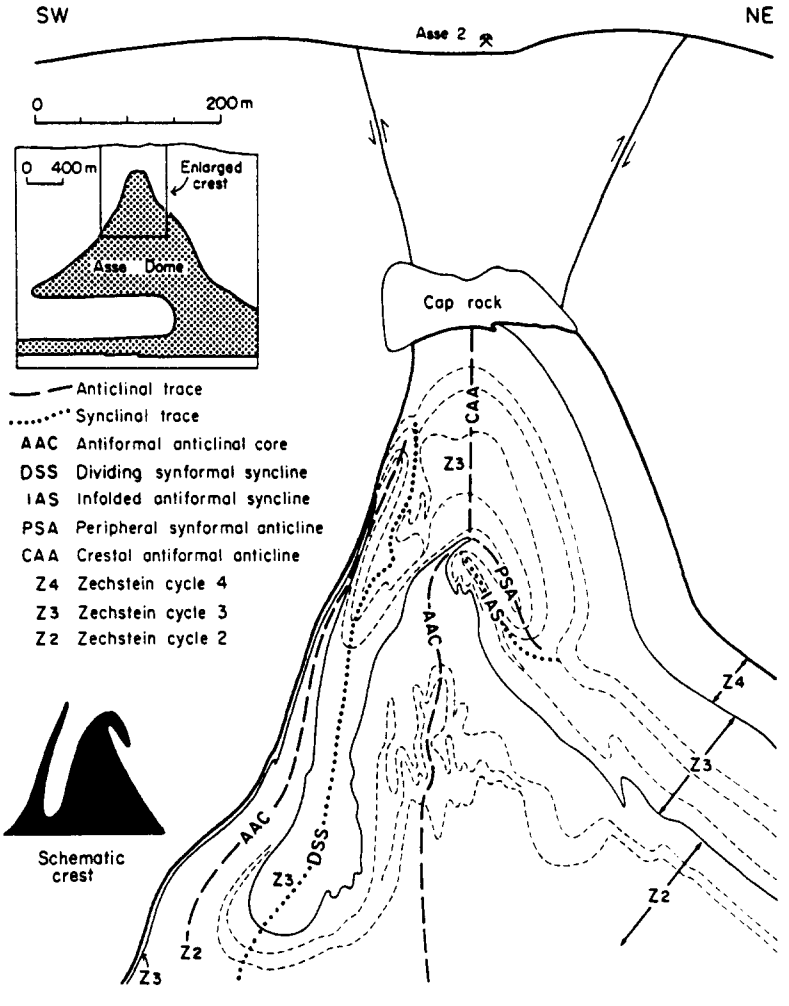

Fig. 15. Vertical section through Asse 2 mine, Asse Dome, a mushroom diapir southeast of Braunschweig, West Germany (adapted from Essaid & Klarr, 1982). Inset shows stippled Zechstein evaporites deformed into an asymmetric mushroom diapir (adapted from Klarr *et al.* 1987). Like the centrifuged diapirs in Figs. 12 and 13, the smooth rounded crestal zone (CAA) of the Asse diapir disguises a complex internal structure enlarged in the main section and shown schematically at lower left. The crest is a fivefold double diapir whose inner part is a threefold asymmetric diapir. A major ductile shear zone has telescoped or removed some Zechstein units and younger units on the southwest.

Gorleben Dome (Fig. 17) is being investigated as a possible site for storage of all types of nuclear waste generated in West Germany (Grübler 1986). Because of its low potash content (Jaritz *et al.* 1986), Gorleben Dome is unmined. Nearly 50 boreholes to the top of the salt define the subcrop of Zechstein units *Z*2–*Z*4 at the dissolution table on the diapir crest (Fig. 17a). But because only six deep boreholes penetrate the diapir bulb, its anatomy—especially in the southeast—is highly speculative. Accordingly, we discuss the merits of three different structural interpretations of Gorleben Dome (Fig. 17c–e). Bornemann (1982) commented on the existence of downward-facing folds in the southeast part of the diapir but apparently did not recognize the mushroom structure.

Figure 17(c) shows the simplest interpretation, a threefold internal simple mushroom diapir comparable to the centrifuged diapir shown in Fig. 8. Supporting this interpretation is a deep boring to the northeast, which indicates that the infold there is cored by *Z*3 and *Z*4 evaporites. However, this interpretation is incompatible with measured stratigraphic thicknesses. Zechstein unit *Z*4 is about 60 m thick (Jaritz *et al.* 1986) Yet the interpretation in Fig. 17(c) requires *Z*4 thickness of several hundred meters, which appears unrealistic, even allowing for strain thickening in fold hinge zones (cf. Fig. 5).

A second interpretation (Fig. 17d) is similar to the first, except that the mushroom structure is external: the infold is cored by country rock. We drew this infold conservatively narrow (although it could be an even narrower, shredded screen of country rock), but a wider infold of cover is clearly one way to reduce the *Z*4 thickness to a realistic value. This interpretation implies that the effective viscosity of the country rocks (Muschelkalk to Lower Cretaceous) is similar to that of the Zechstein evaporites.

A third possibility is an internal vortex structure (Fig. 17e). The space occupied by the inferred vortex reduces the *Z*4 thickness to a realistic value. This interpretation (and its rheologic implications) is supported by the similar internal vortex structure deduced for Hänigsen Dome (Fig. 16), which has much better subsurface control.

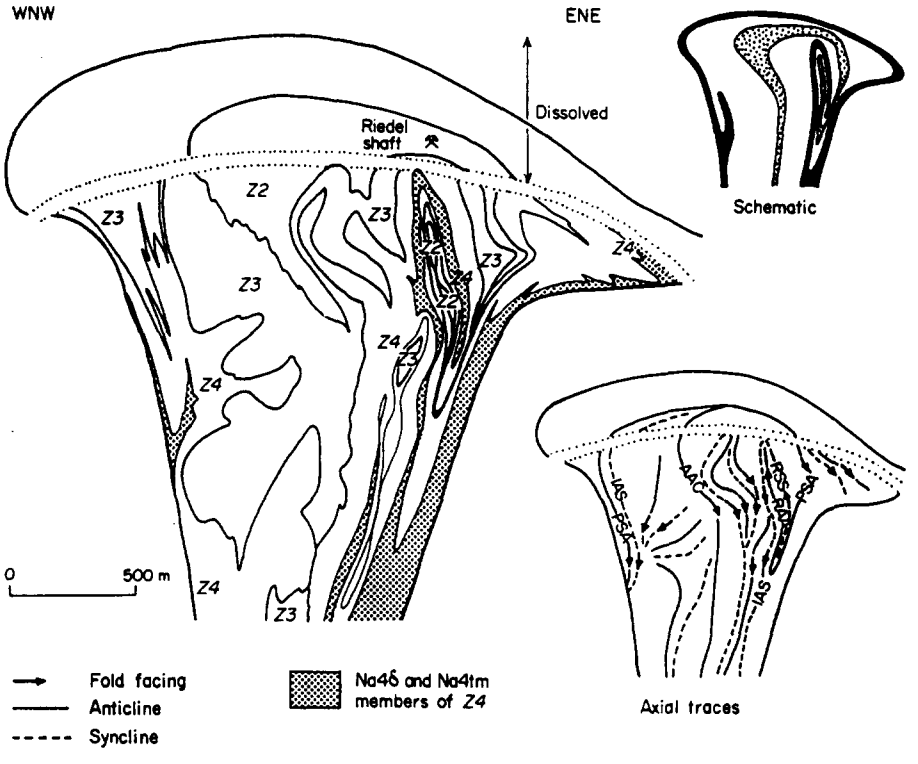

Fig. 16. Vertical section through Riedel mine, Hänigsen Dome, a mushroom diapir northeast of Hanover, West Germany (adapted from Schachl 1987). The symbols Z2, Z3 and Z4 represent Zechstein cycles 2, 3 and 4. The stippled fold (uppermost part of Z4) intersected by the Riedel shaft in the main cross-section is anomalously upward-facing. We therefore interpret it as a reversed antiformal anticline (RAA in axial-trace section), forming part of a vortex structure (see schematic section). AAC, antiformal anticlinal core (out of plane of section in the stem); IAS, infolded antiformal syncline; PSA, peripheral synformal anticline (skirt); RSS, reversed synformal syncline. Fold facing is reliable only in the upper parts of the diapir bulb where fold hinges are subhorizontal.

We favor the latter two interpretations (Fig. 17d & e) over the first (Fig. 17c), but cannot exclude any of the three without further data. Which interpretation is correct has important practical implications (addressed in the Summary).

Other West German diapirs have internal mushroom structure; four are shown in Fig. 18. The slightly elliptical Höfer Dome is a ninefold asymmetric triple diapir defined by Z2, Z3 and Z4 (Fig. 18a). This is only the second example where an infold was previously recognized as an antiformal syncline (Schachl 1968).

Benthe salt wall is famous for its intricate internal convolutions defined by steeply plunging curtain folds and gently plunging anticlines of Z2 trending parallel to the boundary of the intrusion (Stier 1915, Ahlborn & Richter-Bernburg 1953). Some of these ridge-like anticlines have developed small-scale internal mushroom structure (termed *Pilzsattel* by Ahlborn & Richter-Bernburg, 1953). In the east part of the wall, a fivefold internal mushroom diapir (Fig. 18b) has an embayed roof, forming a crestal synformal syncline (CSS) flanked by two crestal antiformal anticlinal (CAA) ridges. The stem is fluted with three vertical buttresses (cf. Fig. 12). The presence of several internal mushroom diapirs about 0.5 km wide within an intrusion 3 km wide indicates that internal toroidal circulation can be confined to only small parts of a diapir.

Other small internal structures have formed within the Aller graben in the Bartensleben mine (Fig. 18c). These threefold structures have a strong and consistent asymmetry, resembling breaking waves caused by salt flow from the southwest up a fault-defined step.

Salzgitterer diapir, a sevenfold asymmetric external double diapir, is even more strongly controlled by regional faults along which it has intruded (Fig. 18d). The folds are upward-facing in the west and downward-facing in the east (Lotze 1957).

Other examples of internal mushroom structures on various scales in the Zechstein basin have been illustrated elsewhere from the Hansa-Silverberg 1 mine, the Wendelstein mine on the Unstrut River (Lotze 1957) and the Deutschland mine at Westfeld (Stier 1915).

U.S. Gulf Coast

Unlike those in West Germany, salt diapirs of the U.S. Gulf Coast generally lack readily correlatable layers because their rock salt is too pure. An exception is Palangana Dome, one of a small group of South Texas diapirs consisting of impure evaporites of unknown age. The mushroom structure of Palangana Dome can be recognized on the basis of the dome's internal stratigraphy defined by potash minerals and logged in deviated boreholes (Hofrichter 1968). Changes in younging direction mapped by Hofrichter and his coworkers indicate that at least four major folds are present in their vertical section. The simplest explanation of this structure is that

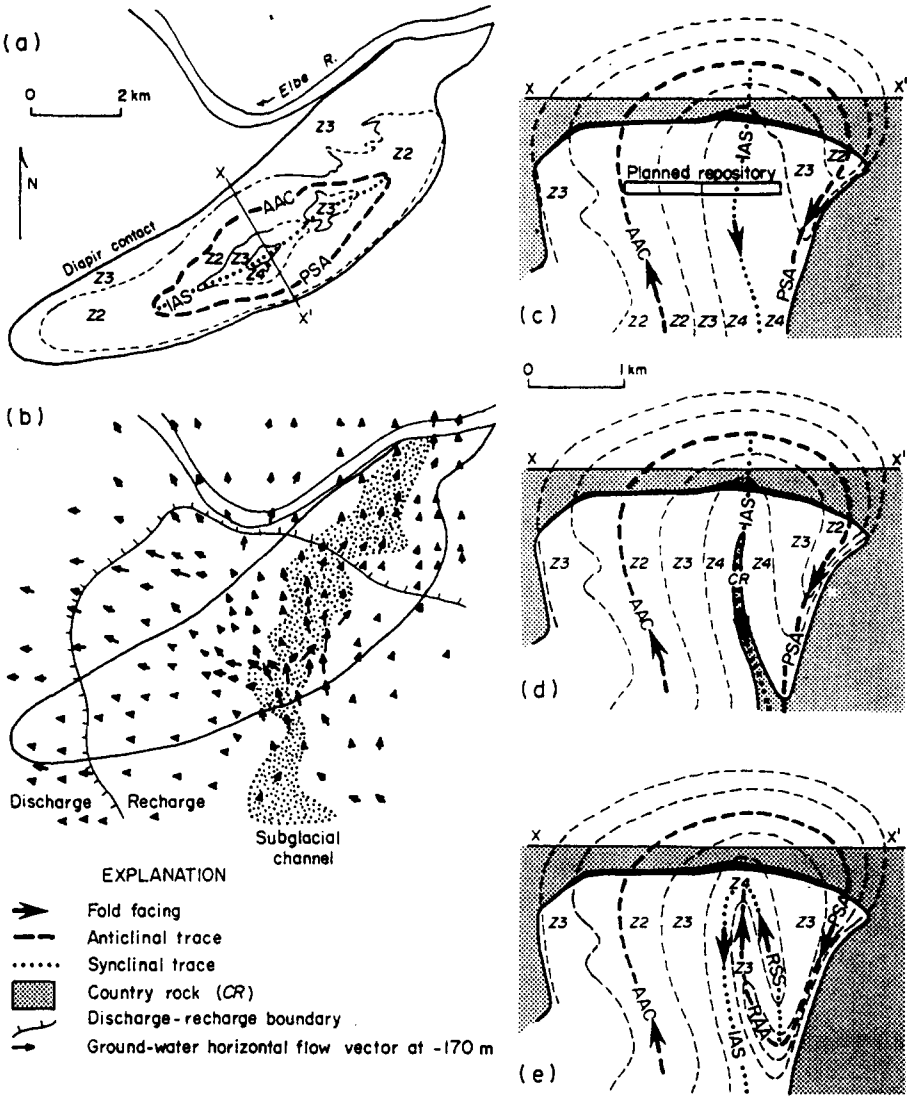

Fig. 17. Maps (a, b) and vertical sections (c–e) of Gorleben Dome, a mushroom diapir between Laase and Trebel, West Germany. (a) Subcrop of Zechstein cycles 2–4 (*Z2*, *Z3*, *Z4*) at the crest of the buried diapir and the axial traces of the simplest structural interpretation: a threefold diapir. (b) Map showing hydrology of the diapir and its surroundings: 100-m-deep subglacial erosion channel (random stipple) cut into cap rock and salt; discharge–recharge boundary based on piezometric head measurements in the shallow aquifer and three-dimensional mathematical modelling in the deep aquifer just above the diapir crest; flow vectors based on the mathematical modelling of the deep aquifer, which assumes constant-density fluids and is therefore approximate. (c) Structural interpretation as a threefold internal mushroom diapir; the planned position of a nuclear waste repository at depths of 840–960 m is after Grübler (1986). (d) Structural interpretation as a threefold external mushroom diapir. (e) Structural interpretation as a fivefold internal mushroom diapir with vortex structure. Area above cap rock (black) has been eroded or dissolved. AAC, antiformal anticlinal core; IAS, infolded antiformal syncline; PSA, peripheral synformal anticline (skirt); RAA, reversed antiformal anticline; RSS, reversed synformal syncline. (a and b adapted from Jaritz *et al.* 1986; c adapted from Bornemann 1982.)

of a fivefold mushroom diapir, as illustrated by Jackson & Talbot (1985) and Talbot & Jackson (1987a).

Many of the Gulf Coast salt domes contain exotic inclusions of shale, sandstone, or carbonate. Some of these inclusions provide indirect, equivocal evidence of mushroom diapirs. Kupfer (1974) drew attention to a screen of Oligocene shale inclusions in Jurassic salt in Belle Isle Dome, Louisiana. The screen, which he termed a "boundary shear zone", appeared to connect the edge of the salt stock to its center. Kupfer (1974) believed that the included shale was derived from above by trapping between two rising tongues of salt. However, on the basis of evidence from our models, it is at least as probable that the shale screen was entrained from below the northwest side as the infold of a mushroom diapir. Perhaps even multiple screens can form either as partitions separating multiple skirts formed by diapiric downbuilding during episodic sedimentation, or as a single infold of country rock attenuated, coiled and duplicated within a vortex mushroom structure.

If the diapir bulb is truncated by subsurface solution of salt, shale inclusions remain because of their insolubility. On reaching the dissolution table at the salt crest, steeply dipping shale inclusions would rotate as they were incorporated into the basal accretion zone of cap rock, and shale and anhydrite would become interstratified in the cap rock. Seni (1987) mapped shale inclusions up to 30 m thick and hundreds of meters wide in the cap rock of

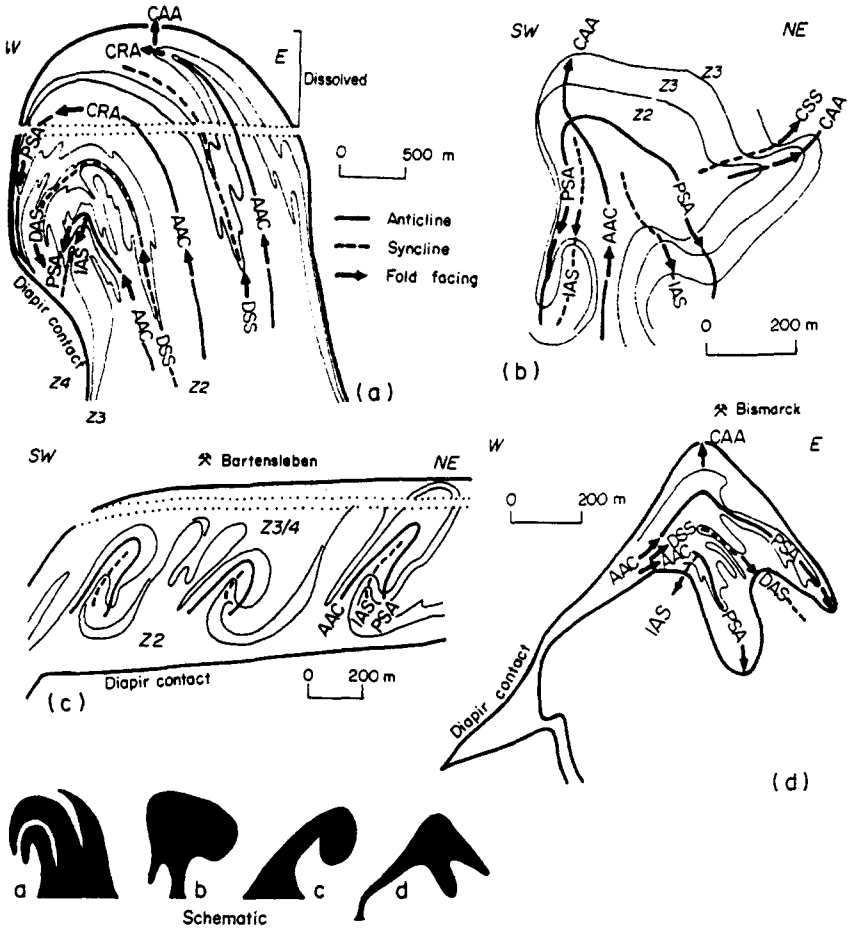

Fig. 18. Vertical sections of four West German salt domes characterized by internal mushroom structure. Z2, Z3 and Z4 represent Zechstein cycles 2, 3 and 4. (a) Höfer Dome, a ninefold triple diapir in the Mariaglück mine northeast of Hanover (adapted from Schachl 1968). (b) A small fivefold internal mushroom diapir in Ronnenberg mine in the Benthe salt wall, a composite diapir at Hanover (adapted from Ahlborn & Richter-Bernburg 1953). (c) Small threefold internal mushroom diapirs in Bartensleben mine in the Aller graben (adapted from Richter-Bernburg 1980). (d) Sevenfold double diapir intruded along a regional fault in Bismarck mine in Salzgitterer Dome at Salzgitter (adapted from Lotze 1957). AAC, antiformal anticlinal core; CAA, crestal antiformal anticline; CRA, crestal recumbent anticline; DAS, dividing antiformal syncline; DSS, dividing synformal syncline; IAS, infolded antiformal syncline; PSA, peripheral synformal anticline (skirt). The area above the double dotted lines in (a) and (c) has eroded or dissolved.

Boling Dome, Texas. He suspected that they were derived from inclusions within the now-eroded part of the salt stock.

Canadian Arctic Islands

Exposed diapirs in the Sverdrup Basin of the Canadian Arctic (Tozer & Thorsteinsson 1964, Schwerdtner & Osadetz 1983, van Berkel 1986) consist of upper Carboniferous anhydrite, non-evaporite inclusions and rare rock salt at the present level of erosion; presumably salt is the main constituent of diapirs below the surface. The anhydrite of Barrow Dome (Fig. 19a) encloses a crescent of mafic plutonic rocks.

Figures 19(b)–(d) show successive stages of emplacement of evaporites and country rock to form a composite diapir by a process of 'balloon tectonics'. Conceivably, this process could form the crescent shown in Fig. 19(a), but it is unlikely that a crescent of mafic plutonite could be emplaced diapirically in the manner shown because the rock is too dense.

An alternative hypothesis is that dense plutonite was dragged up by underlying or enclosing evaporites. The crescent of mafic plutonite probably represents an originally planar overburden tightly infolded by diapirism of the evaporite source layer. The vertical sections (Figs. 19e & f) illustrate why the mafic rocks form a crescent rather than a ring. The inner area of radial curtain folds represents a core, whereas the outer area of concentric folds represents a skirt, illustrating our thesis that curtain folds are unfolded, or rotated and tightened, as they move out of the stem or bulb core into the bulb crest and periphery. The diapir thus appears to have external mushroom structure. A problem with this interpretation is why the effective viscosity of the mafic rock was low enough for it to be entrained into a mushroom structure.

Central Iran

The detailed internal structure of more than 50 Tertiary salt diapirs superbly exposed in the Great Kavir of

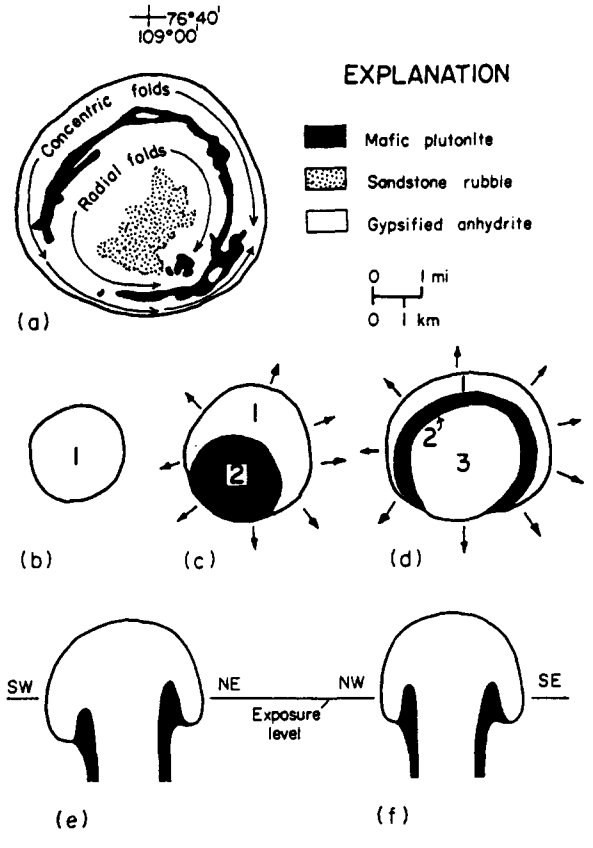

Fig. 19. Barrow Dome, a diapir of gypsified anhydrite and mafic plutonite exposed on Melville Island in the Sverdrup Basin, Canadian Arctic. (a) Map of the dome from Tozer & Thorsteinsson (1964) and Schwerdtner & Osadetz (1983). (b) An interpretation for the emplacement of the composite diapir by balloon tectonics viewed in a time sequence in horizontal section. (c) A more realistic interpretation in vertical section in which the mafic rock is an infold of cover dragged up by the evaporite.

Central Iran is currently being studied (Jackson & Cornelius 1985, Jackson *et al.* 1987). During diapirism, Eocene–Oligocene rock salt, informally termed the Older Salt, entrained its Oligocene–Miocene cover, informally termed the Younger Salt (Stöcklin 1968). This cover is a strongly banded, variegated suite of evaporites (including rock salt) and lacustrine-facies clastic rocks. No subsurface structural data are available.

Both Kavir examples shown in Fig. 20 have external mushroom structure. Dome 20 has a core of Older Salt surrounded by an infolded ring of Younger Salt, which in turn is rimmed by a skirt of Older Salt. Bedding traces within the Younger Salt (not shown) indicate that the antiformal ring plunges toward a depression in the southwest; the dome is higher in the northeast because it is joined to a twin diapir (Fig. 20, section C–C').

Dome 14 also leans to the southwest and its antiformal infold of Younger Salt plunges beneath the surface (Fig. 20, section E–E'), forming a crescent (rather than a ring) as in Barrow Dome (Fig. 19). Dome 14 (Fig. 20) is one of three external vortex mushroom diapirs in the Kavir. The map of dome 14 shows a hook of Younger Salt enclosing Older Salt in the south; bedding traces in the west (not shown) also delineate a hook, except that it encloses Younger Salt (Fig. 20, section D–D'). These hooks represent the inwardly rolled-up margins of the diapir bulb.

SOME DYNAMIC CONSIDERATIONS

Nature of diapiric contacts

Except where salt is juxtaposed against a solution front, the internal structures of creeping salt masses are almost invariably comformable with their contacts. This concordance is visible in salt mines in Germany and the U.S. Gulf Coast and in surface exposures of salt glaciers (Talbot 1979, 1981, Talbot & Jarvis 1984) and salt diapirs (Zak & Freund 1980, Jackson & Cornelius 1985, Jackson *et al.* 1987) in Israel and Iran.

The character of the contact zone of diapirs is obviously scale-dependent, and there are complete gradations between the following: (1) concordant, ductile deformation of both source and cover in a broad zone; (2) a contact zone defined by a ductile shear zone; (3) a discordant contact due to faulting, salt-dike intrusion, or an angular unconformity between sediments and the underlying evaporites.

A faulted contact discordant to both diapir and cover requires a completely rigid diapir, which is unrealistic. However, a combination of (2) and (3) is probably common: inward from the contact, the strain is ductile within the diapir; outward from the contact, the strain could be almost completely brittle in stiff cover rocks such as carbonates. For example, the Mount Sedom diapir in the Dead Sea rift has ductile strains of 2.1–1.7 in the evaporites near the contact, but strain is concentrated as faults in the Pleistocene carbonate, sulfate and clastic cover sediments (Zak & Freund 1980). Similarly, the carbonate cover around the Zagros diapirs in southern Iran is bounded by fault zones having minimal ductile strain.

In summary, field data suggest that high ductile strains characterize the diapir side of the contact zone, but that—not surprisingly—the country rock deformation style depends on lithology. Our centrifuged models appear to be applicable to all diapirs that intrude relatively ductile rocks, such as incompletely lithified terrigenous clastics or gneisses at amphibolite-grade conditions. Ductility of the immediate cover is required for the formation of external mushroom diapirs, so the centrifuge results apply to any natural diapir of this form.

Effective viscosity contrast

Estimates of the effective viscosity of dry rock salt vary widely from 10^{15} to 10^{20} Pa s (LeCompte 1965, Heard 1972, Carter & Hansen 1983). This variation results from the effects of experimental work hardening as well as varying factors of temperature, differential stress, strain rate, grain size, water content and whether the deforming specimen is allowed to dilate. Traces of water lower the effective viscosity of salt by orders of magnitude and allow it to behave more like a Newtonian

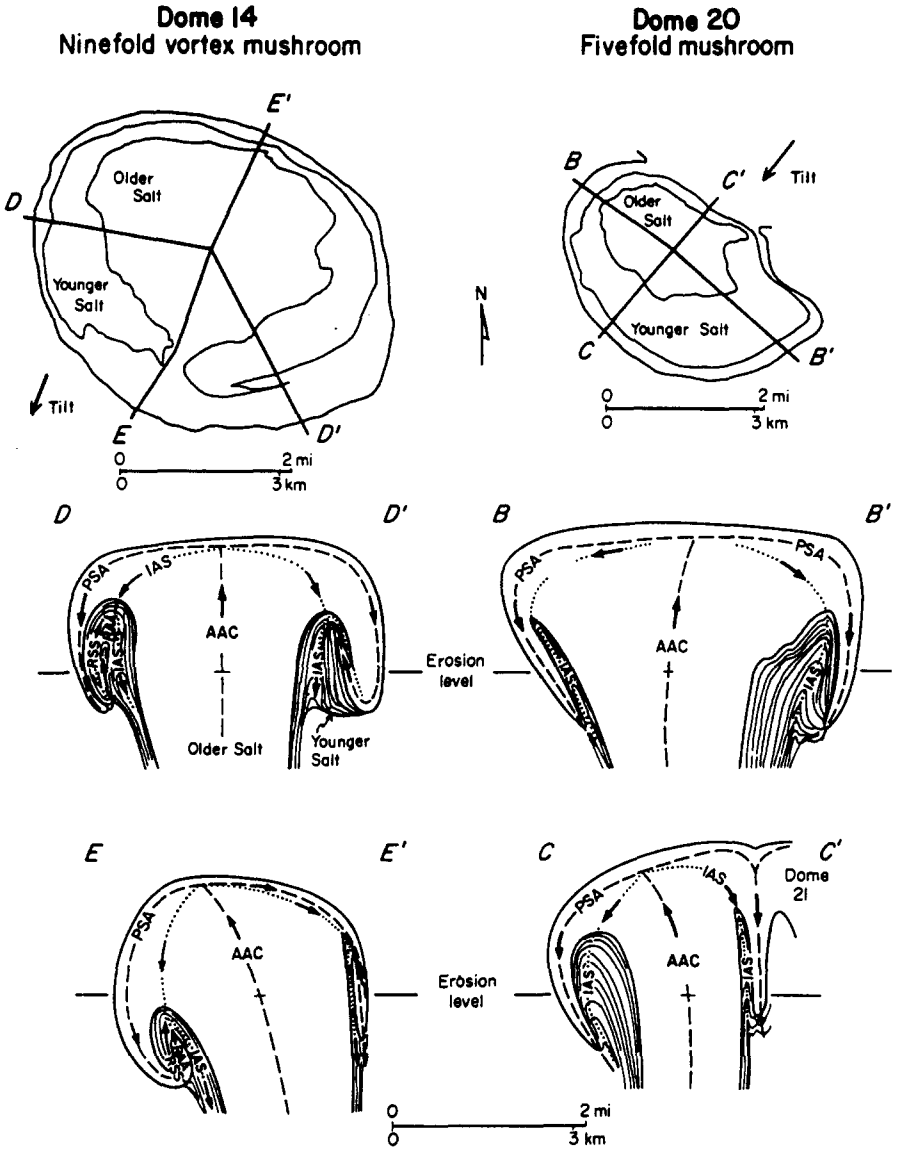

Fig. 20. Vertical sections through two external mushroom diapirs in the Great Kavir, Central Iran. Maps at the top of each column show the lines of section. Dome 14 is a ninefold vortex mushroom diapir. Dome 20 is a fivefold mushroom diapir joined to Dome 21, a Siamese twin. Arrows in vertical sections show fold facing. AAC, antiformal anticlinal core; IAS, infolded antiformal syncline; PSA, peripheral synformal anticline (skirt); RAA, reversed antiformal anticline; RSS, reversed synformal syncline. (From Jackson *et al.* 1987.)

fluid than does dry rock salt (Spiers *et al.* 1986, Urai *et al.* 1986).

The absolute viscosities of terrigenous clastic sediments are much less known. Apart from certain other evaporite minerals (sylvite, carnallite and bischofite), lithified beds of other rock types generally have buckled or boudinaged in naturally deformed rock salt. This indicates that rock salt has a lower viscosity than most other lithified nonevaporite rocks (Richter-Bernburg 1987). The effective viscosity of an overburden is clearly time and space dependent. Newly deposited clastic sediments have lower effective viscosities than crystalline rock salt. As clastic rocks become lithified during burial, the effective viscosity of the immediate cover increases toward, becomes equal to, then (with the possible exception of overpressured shale) increases above the effective viscosity of salt. So at some stage the condition $0.1<m<10$ should approximate, which gives rise to external mushroom diapirs, later modified to internal mushroom diapirs as m rises with consolidation (Fig. 1). Diapirs growing through already consolidated overburdens may evolve solely along the path to internal mushroom structures.

Although mushroom bulbs are therefore to be expected in nature on the basis of theory and experiment, salt diapirs are typically portrayed as thumb shaped (Fig. 1, $m \ll 1$), which we would expect only if diapir bulbs matured rapidly before their immediate cover had time to lithify significantly. There are three possible reasons for this bias toward drawing thumb-shaped diapirs. First, deep boreholes close to the center of a dome are rare, so the interpreter may conservatively assume the bulb is simpler and the stalk is wider than they really are. Second, the misleading effects of seismic shadow mask the region below the overhang and produce an apparent thumb shape (Tucker & Yorston 1973,

example 13), although as migration techniques improve, definition of the overhang also improves (Withjack *et al.* 1986). Third, the diapirs may be too immature to have formed a broad bulb.

SUMMARY: MUSHROOM DIAPIRS AND THEIR IMPLICATIONS TO ENGINEERING AND PETROLEUM EXPLORATION

External mushroom diapirs form where the cover has similar effective viscosity to the diapiric material. Toroidal circulation includes the cover, the diapiric contact is infolded as part of the mushroom structure, and the infold is cored by the cover.

Internal mushroom diapirs form where the cover has significantly higher viscosity than the diapiric material. Toroidal circulation is confined to the diapiric material in the bulb and no cover is entrained. The diapiric contact is not infolded, the mushroom structure is contained entirely within the diapir, and the infold is cored by the diapiric material. In both internal and external mushroom diapirs, skirts can curl inward to form vortices capable of entraining cover material to varying degrees.

We have illustrated several examples, but there is not enough information to be confident of the internal structure of more than a tiny proportion of the world's salt diapirs. External mushroom diapirs may be comparatively rare in nature, although they would be difficult to recognize if they have narrow skirts. Only some diapirs mature to the stage of a wide overhanging bulb of any sort. Only where the cover rocks are of similar effective viscosity to the diapiric rocks can a mature bulb have an external skirt. These conditions are probably limited to four zones: (1) at depths where the cover viscosity has reached transient similarity to the diapir viscosity through progressive lithification; (2) where the cover rocks themselves contain evaporites, as in Central Iran; (3) where the cover is overpressured shale; and (4) where gneisses are overlain by denser metamorphites under amphibolite-facies conditions. Possibly only the immediate cover need have viscosity similar to that of the diapir for an external skirt to form. The minimum thickness of this isoviscous cover may be that which can be enclosed by the diapir skirt.

In contrast, internal mushroom diapirs consist entirely of diapiric material, so conditions of isoviscosity are automatically satisfied within their bulbs. Thus internal mushroom shapes are expected to be relatively common, as shown in our examples.

The possibility of external mushroom diapirs in nature has important implications for any engineering in a salt dome, including nuclear waste storage. The degree of concern depends upon the hydrogeology of the infold. A completely internal infold (Figs. 2, 15 and 18a–c) consists entirely of evaporites and is not an avenue of enhanced permeability. The infold of an external mushroom diapir is cored by cover (Figs. 2, 19 and 20), which may be more permeable than the diapiric material. These zones of potentially enhanced permeability may connect not only to the country rocks below but also to a solution surface above.

For this reason, the possible existence of infolded country rock in the southeastern part of Gorleben Dome in West Germany is highly relevant (Fig. 17d). It is planned to store all types of nuclear waste in this dome. A subglacial erosion channel was cut obliquely across the Gorleben crest through the cap rock and into the salt (Fig. 17b). Ground water flowing north is recharged over the dome, and flow (at a rate of > 10 m a^{-1}) is concentrated in the erosion channel before discharging at the northeast end of the diapir. The density and salinity of the ground water increase northeastward, suggesting dissolution of the dome through the window of glacially eroded cap rock. Significantly, the dissolution zone in the eroded channel overlies the infold. If the infold is cored by cover (Fig. 17d), the planned repository site in Gorleben Dome may be intersected by a possible hydrologic connection from the deepest part of the overhang to the surface where salt is being dissolved in the subglacial channel. Given the need to limit deep drilling through the planned storage area for nuclear waste, the possible existence of permeable country rock deep inside the salt wall can be excluded only by the excavations in progress.

Because the engineering implications of external mushroom diapirs focus on the screens of country rock within a diapir, their recognition is critical. With increasing finite strain, the screen of country rocks progressively thins and may be dismembered by boudinage or fracture and duplicated by isoclinal folding to the point where its connection with the exterior is no longer obvious. However, the search for infolds of country rock can be focused on particular salt diapirs that show evidence of being mushroom shaped. Some of the criteria outlined below for detecting infolds rely on exploration techniques such as three-dimensional seismic reflection, vertical seismic profiling, radar, directional drilling and subsurface excavation.

Any mushroom structure is likely to be obscure in undrilled, buried diapirs. External mushroom shapes (and, hence, screens) should be suspected wherever the effective viscosity of any of the pierced overburden layers could have been similar to that of the salt at the time of the bulb growth. Given the distinctive crescentic or ring shape of the infold of country rock, this might be imaged as an anomaly on maps of gravity and aeromagnetics. Skirts or flanges of salt are also potentially visible using geophysical remote sensing; any screens of country rock would form the inner flank of the skirts.

Stratigraphic, folding and fabric criteria can be applied if the interior of the diapir is exposed at the surface or has been drilled or excavated. The stratigraphic approach requires correlatable internal units within the diapir. Screens of infolded country rock are younger than the diapiric evaporite sequence, so they lie at the highest stratigraphic (not structural) level in the diapir. If the relative ages of the evaporites are unknown, screens should be suspected along any sur-

faces of stratigraphic symmetry, some of which may coincide with isoclinal infolds.

Three clues related to folding should alert the structural geologist to the possibility of mushroom structure: large crescentic infolds, downward-facing folds and, most diagnostic of all, the occurrence of an outer rim of the oldest diapiric member. If the internal stratigraphy is known, anticlines can be differentiated from synclines, and fold facing can be determined. Some rules of fold interpretation are helpful. In our experiments the outermost crescentic fold was invariably anticlinal regardless of its facing direction. The core can be located near the center or edge of a diapir in horizontal section; its location is an unreliable criterion for identification. Differentiation between the diapir core and the skirt requires particular care in horizontal sections, because both are anticlines. The diapir core invariably contains the oldest unit in that particular plane of section. Once any of the three folding clues has been recognized, potential screens should be sought along the axial surface of the infolds, which may be close to isoclinal. Some screens are circumferential and parallel to the external contacts on the sides of the diapir; other screens can be deformed by curtain folding, especially close to the diapir core where curtain folding is strongest. If part of a screen is found, it should be followed in case it coils deeper inside the diapir via a vortex. Any coiling of the screen is most likely to be around subhorizontal axes.

Finally, the grain-shape fabrics can provide another three clues (Talbot & Jackson 1987a). First, steeply plunging linear fabrics indicate either a truncated stem or the core of an axisymmetric bulb. Neither of these zones is likely to have screens of included country rock. Thus, other factors being equal, zones where grain fabrics are uniformly prolate and vertical will provide the least engineering challenges. Second, shallowly dipping planar fabrics indicate the crest of a bulb, which is commonly truncated by dissolution. Third, steeply dipping planar fabrics, particularly where associated with clastic screens, should prompt suspicion that they represent the originally outer parts of the bulb, now intensely smeared by infolding—perhaps even coiling—within the diapir. Screens of country rock are expected to be subparallel to the foliation of the enclosing salt.

The shape of mushroom diapirs is significant to petroleum exploration because such diapirs hide volumes of reservoir rock that would normally be written off in exploration. A seismic shadow below the diapir overhang could conceal cover rocks overhung by a type C (internal mushroom) bulb; here the trap is supplied by the contact aureole of updragged strata against the salt seal. Alternatively the cover rocks could be arched into the infold of a type B (external mushroom) bulb; here the trap is the antiformal infold, again sealed against salt. In mushroom bulbs that have spread laterally to form sheet-like flanges, the infolds could represent very broad antiformal traps. Any fracturing of the infolded cover would enhance secondary porosity and, hence, the prospectivity of the structure.

Acknowledgements—Research was supported by the U.S. Department of Energy Salt Repository Project Office under contract No. DE-AC97-83WM46651. The conclusions of the authors are not necessarily endorsed or approved by the Department of Energy. Hans Ramberg, Ruud Weijermars, Peter Rönnlund and Pierre Heeroma (University of Uppsala) provided helpful suggestions and comments during our experiments. Ronald Arvidsson (University of Uppsala) assisted greatly in material preparation and testing and model construction. Reinold Cornelius (Bureau of Economic Geology) prepared most of the vertical and horizontal section diagrams of centrifuged domes and the block diagram derived from these sections and also provided valuable suggestions. Werner Jaritz supplied us with recent papers on Asse, Gorleben and Hänigsen diapirs. We thank Steven Martel, John Dixon and Jake Hossack for their helpful comments on the manuscript. Figures were drafted by Jana Brod, Margaret L. Evans, Jamie A. McClelland, Nan Minchow-Newman and Kerza A. Prewitt, under the supervision of Richard L. Dillon, and by the authors. Publication authorized by the Director, Bureau of Economic Geology, The University of Texas at Austin.

REFERENCES

Ahlborn, O. & Richter-Bernburg, G. 1953. Exkursion zum Salzstock von Benthe (Hannover), mit Befahrung der Kaliwerke Ronnenberg und Hansa. *Z. dt. geol. Ges.* **105**, 855–865.

Balk, R. 1949. Structure of Grand Saline salt dome, Van Zandt County, Texas. *Bull. Am. Ass. Petrol. Geol.* **33**, 1791–1829.

Berner, H., Ramberg, H. & Stephansson, O. 1972. Diapirism in theory and experiment. *Tectonophysics* **15**, 197–218.

Bornemann, O. 1982, Stratigraphie und Tektonik des Zechsteins im Salzstock Gorleben auf Grund von Bohrergebnissen. *Z. dt. geol. Ges.* **133**, 119–134.

Carter, N. L. & Hansen, F. D. 1983. Creep of rocksalt. *Tectonophysics* **92**, 275–333.

Daly, B. J. 1967. Numerical study of two fluid Rayleigh–Taylor instability. *Physics Fluids* **10**, 297–307.

Dixon, J. M., 1975. Finite strain and progressive deformation in models of diapiric structures. *Tectonophysics* **28**, 89–124.

Escher, B. G. & Kuenen, P. H. 1929. Experiments in connection with salt domes. *Leid. geol. Meded.* **3**, 151–182.

Essaid, S. & Klarr, K. 1982. Zum Innenbau der Salzstructur Asse. *Z. dt. geol. Ges.* **133**, 135–154.

Grübler, G. 1986. Programme for investigating the suitability of the Gorleben salt dome as a repository for radioactive waste. In: *Siting, Design and Construction of Underground Repositories for Radioactive Wastes*. International Atomic Energy Agency, Vienna, IAEA-SM-289/43, 363–369.

Heard, H. C. 1972. Steady-state flow in polycrystalline halite at pressure of 2 kilobars. In: *Flow and Fracture of Rocks* (edited by Heard, H. C., Borg, I. Y., Carter, N. L. & Raleigh, C. B.). *Am. Geophys. Un. Geophys. Monogr.* **16**, 191–210.

Heye, D. 1978. Experimente mit viskosen Flussigkeiten zur Nachahmung von Salz strukturen. *Geol. Jb.* **E12**, 31–51.

Heye, D. 1979. Modellversuche zum Salzdiapirismus mit viskosen Flussigkeiten. *Geol. Jb.* **E16**, 39–51.

Hofrichter, E. 1968. Stratigraphy and structure of the Palangana salt dome, Duval County, Texas. *Spec. Pap. geol. Soc. Am.* **88**, 365–379.

Jackson, M. P. A. 1985. Natural strain in diapiric and glacial rock salt, with emphasis on Oakwood Dome, East Texas. *Univ. Texas at Austin Bur. Econ. Geol. Rept Investigations* 143.

Jackson, M. P. A. & Cornelius, R. R. 1985. Tertiary salt diapirs exposed at different structural levels in the Great Kavir, Central Iran: a remote-sensing study of their internal structure and shape. *Univ. Texas at Austin Bur. Econ. Geol, Rept for U.S. Dept. Energy.*

Jackson, M. P. A. & Cornelius, R. R. 1987. Stepwise centrifuge modeling of the effects of differential sedimentary loading on the formation of salt structures. In: *Dynamical Geology of Salt and Related Structures* (edited by Lerche, I. & O'Brien, J. J.). Academic Press, Orlando, 163–259.

Jackson, M. P. A., Cornelius, R. R., Craig, C. H., Gansser, A., Stöcklin, J. & Talbot, C. J. 1987. Geology and dynamics of a salt diapir province in the Great Kavir, Central Iran. *Univ. Texas at Austin Bur. Econ. Geol Open File Rept* OF-WTWI-1987-04.

Jackson, M. P. A. & Talbot, C. J. 1985. Reinterpretation of the internal structure of Palangana salt dome, South Texas. *Bull. South Texas geol. Soc.* **25**, 37–48.

Jackson, M. P. A. & Talbot, C. J. 1986. External shapes, strain rates, and dynamics of salt structures. *Bull. geol. Soc. Am.* **97**, 305–323.

Jackson, M. P. A., Talbot, C. J. & Cornelius, R. R. 1988. Centrifuge modeling of the effects of aggradation and progradation on syndepositional salt structures. *Univ. Texas at Austin Bur. Econ. Geol. Rept Investigations* 173.

Jaritz, W., Bornemann, O., Giesel, W. & Vierhuff, H. 1986. Geoscientific investigation of the Gorleben site. In: *Siting, Design and Construction of Underground Repositories for Radioactive Wastes*. International Atomic Energy Agency, Vienna, IAEA-SM-289/44, 371–384.

Klarr, K., Richter-Bernburg, G. & Rothfuchs, T. 1987. Schachtanlage Asse der Gesellschaft für Strahlen- und Umweltforschung mbH, München. Der Zechstein der Asse südöstlich Braunschweig und geowissenschaftliche Versuche der Endlagerung hochradioaktiver Abfälle. In: *International Zechstein Symposium* 1987, *Excursion Guide* I. Kulick and Paul. Wiesbaden, 101–122.

Kupfer, D. H. 1968. Relationship of internal to external structures of salt domes. In: *Diapirism and Diapirs* (edited by Braunstein, J. & O'Brien, G. D.). *Mem. Am. Ass. Petrol. Geol.* **8**, 79–89.

Kupfer, D. H. 1974. Boundary shear zones in salt rocks. In: *Fourth Symposium on Salt* (edited by Coogan, A. H.). *Northern Ohio geol. Soc.* **1**, 215–225.

LeCompte, P. 1965. Creep in rock salt. *J. Geol.* **73**, 469–484.

Lotze, F. 1957. *Steinsalz und Kalisalze, Teil* 1, *Allgemein-Geologischer Teil* (2nd Edn). Gebrüder Borntraeger, Berlin.

Ramberg, H. 1981. *Gravity, Deformation and the Earth's Crust in Theory, Experiments and Geological Application* (2nd Edn.). Academic Press, London.

Richter-Bernburg, G. 1980. Salt tectonics: interior structures of salt bodies. *Bull. Cent. Rech. Explor. Prod. Elf-Aquitaine* **4**, 373–393.

Richter-Bernburg, G. 1987. Deformation within salt bodies. In: *Dynamical Geology of Salt and Related Structures* (edited by Lerche, I. & O'Brien, J. J.). Academic Press, Orlando, Florida, 39–75.

Schachl, E. 1968. Mine Mariaglück, Höfer. *International Symposium of the Geology of Saline Deposits, Excursion Guide*. Bundesanstalt für Bodenforschung, Hanover.

Schachl, E. 1987. Exkursion G. Kali- und Steinsalzbergwerk Niedersachsen-Riedel der Kali und Salz AG, Schachtanlage Riedel—Zechsteinstratigraphie und Innenbau des Salzstockes von Wathlingen-Hänigsen. In: *International Zechstein Symposium* 1987, *Excursion Guide* I. Kulick and Paul, Wiesbaden, 69–100.

Schmeling, H. 1987. On the relation between initial conditions and late stages of Rayleigh-Taylor instabilities. *Tectonophysics* **133**, 16–31.

Schmeling, H., Cruden, A. R. & Marquart, G. 1988. Finite deformation in and around a fluid sphere moving through a viscous medium: implications for diapiric ascent. *Tectonophysics* **149**, 17–34.

Schwerdtner, W. M. & Osadetz, K. 1983. Evaporite diapirism in the Sverdrup Basin: new insights and unsolved problems. *Bull. Can. Petrol. Geol.* **31**, 27–36.

Seni, S. J. 1987. Evolution of Boling Dome cap rock with emphasis on included terrigenous clastics, Fort Bend and Warton Counties, Texas. In: *Dynamical Geology of Salt and Related Structures* (edited by Lerche, I. & O'Brien, J. J.). Academic Press, Orlando, Florida, 543–591.

Spiers, C. J., Urai, J. L., Lister, G. S., Boland, J. N. & Zwart, H. J. 1986. The influence of fluid-rock interaction on the rheology of salt rock. *Nuclear Science and Technology, CEC-EUR* 10399 *EN*.

Stier, K. 1915. Strukturbild des Benther Salzgebirges. *Jber. niedersächs. geol. Ver.* **8**, 1–14.

Stöcklin, J. 1968. Salt deposits of the Middle East. *Spec. Pap. geol. Soc. Am.* **88**, 158–181.

Talbot, C. J. 1974. Fold nappes as asymmetric mantled gneiss domes and ensialic orogeny. *Tectonophysics* **24**, 259–276.

Talbot, C. J. 1977. Inclined and asymmetric upward-moving gravity structures. *Tectonophysics* **42**, 159–181.

Talbot, C. J. 1979. Fold trains in a glacier of salt in southern Iran. *J. Struct. Geol.* **1**, 5–18.

Talbot, C. J. 1981. Sliding and other deformation mechanisms in a glacier of salt, S. Iran. In: *Thrust and Nappe Tectonics* (edited by McClay, K. R. & Price, N. J.). *Spec. Publs geol. Soc. Lond.* **9**, 173–183.

Talbot, C. J. & Jackson, M. P. A. 1987a. Internal kinematics of salt diapirs. *Bull. Am. Ass. Petrol. Geol.* **71**, 1068–1093.

Talbot, C. J. & Jackson, M. P. A. 1987b. Salt tectonics. *Sci. Am.* **256**, No. 2, 70–79.

Talbot, C. J. & Jarvis, R. J. 1984. Age, budget and dynamics of an active salt extrusion in Iran. *J. Struct. Geol.* **6**, 521–533.

Tozer, E. T. & Thorsteinsson, R. 1964. Western Queen Elizabeth Islands, Arctic Archipelago. *Mem. geol. Surv. Can.* **332**.

Tucker, P. M. & Yorston, H. J. 1973. Pitfalls in seismic interpretation. *Soc. Explor. Geophys. Monogr.* 2.

Urai, J. L., Spiers, C. J., Zwart, H. J. & Lister, G. S. 1986. Weakening of rock salt by water during long-term creep. *Nature, Lond.* **324**, 554–557.

van Berkel, J. T. 1986. A structural study of evaporite diapirs, folds and faults, Axel Heiberg Island, Canadian Arctic Islands. *Amsterdam Univ. GUA Papers of Geology Ser.* 1.

van Dyke, M. 1982. *An Album of Fluid Motion*. Parabolic Press, Stanford.

Whitehead, J. A., Jr & Luther, D. S. 1975. Dynamics of laboratory diapir and plume models. *J. geophys. Res.* **80**. 705–717.

Withjack, M., Reinke-Walter, J., Meisling, K. & Correa, P. 1986. *Seismic Expression of Structural Styles*. ARCO Oil & Gas Co., Plano Texas.

Woidt, W.-D. 1978. Finite element calculations applied to salt-dome analysis. *Tectonophysics* **50**, 369.

Woidt, W.-D. 1980. *Analytische und Numerische Modellexperimente zur Physik der Salzstock Bildung*. Institut für Geophysik und Meteorologie der Technischen Universitat Braunschweig GAMMA 38.

Zak, I. & Freund, R. 1980. Strain measurements in eastern marginal shear zone of Mount Sedom salt diapir, Israel. *Bull. Am. Ass. Petrol. Geol.* **64**, 568–581.